



OCEAN ENGINEERING
TEXAS A&M UNIVERSITY

Microbially-Induced Calcium Carbonate Precipitation (MICP) Supporting Nearshore Dellanera Reef Design for Galveston Island

Final Report

Prepared by

Jens Figlus (Department of Ocean Engineering, Texas A&M University / TEES)

Manoj Kamalanathan (Department of Marine Biology, Texas A&M University at Galveston)

Jaclynn Turnbaugh (Department of Ocean Engineering, Texas A&M University / TEES)

Prepared for

U. S. Army Corps of Engineers – Galveston District (SWG) with funding provided under
Cooperative Ecosystem Studies Unit (CESU) agreement No. W912HZ-17-2-0023 to Texas A&M
Engineering Experiment Station (TEES)

February 2022

Table of Contents

Acknowledgements	5
1 Introduction	6
1.1 Background.....	6
1.2 Literature review.....	7
1.3 Motivation and objectives	11
2 Laboratory Experiments	13
2.1 Development of test protocols	13
2.2 Methods	16
2.3 Results.....	17
2.4 Discussion	20
3 Field Testing	23
3.1 Setups and locations	23
3.2 Methods	28
3.3 Results.....	31
3.4 Discussion.....	36
4 Coastal Engineering Applications of MICP	38
4.1 Geofabric bags	38
4.2 Rock slope stability	41
5 Hydrodynamics and Sediment Analysis	46
6 Conclusions and Recommendations	53
7 References	56

Table of Figures

Figure 2-1: Photo of syringe test setup exploring an alternate layering approach.....	15
Figure 2-2: Experimental setup of cylindrical mesh molds submerged in MICP solution. Molds were created from wire mesh and were filled with autoclaved and natural sand from Dellanera Beach.....	16
Figure 2-3: Growth of <i>S. pasteurii</i> in marine broth (MB) and different concentrations of yeast extract (YE) with 1% glucose.	18
Figure 2-4: Calcification and growth in 20 mg/L yeast extract (S1).	19
Figure 2-5: Growth of <i>S. pasteurii</i> using S1 combined with different S2 options.....	19
Figure 2-6: Growth medium pH value under S1 and different S2 options.	20
Figure 3-1: Photos of test pods with sediment filled to the top (left) and at grade (right).....	23
Figure 3-2: Photos of two different MICP solution delivery systems for field experiments. The left panel shows the pump, hose, and nozzle setup. The right panel displays the graduated manual sprayer containers being filled with MICP solution prior to a field test.....	24
Figure 3-3: Overview map showing field experiment locations on the TAMUG campus and on the beach at the end of the Galveston seawall near Dellanera RV park.	26
Figure 3-4: Planview of project area and field pod locations (yellow square) near Dellanera RV Park on Galveston Island just west of the western end of the seawall. The mean low and mean high tide lines in the vicinity of the project site are shown by green and magenta lines, respectively.	27
Figure 3-5: Cross-shore profiles at the project site and corresponding photo (looking west) of the beach and dune scarp. Field pod site locations are indicated by the purple squares.	27
Figure 3-6: Photos of raised-bed pod setups on the TAMUG campus. Left: Day 1 also showing the solution application system. Right: Field plot on day 22 after initial setup.	29
Figure 3-7: Photo of pod setup used in the second beach test series.	30
Figure 3-8: Comparison of resistive strength of the surface sediment to normal stress (penetrometer) for treatments including S2 with glucose (blue) and fructose (red), respectively, starting from Day 12 after commencement of MICP treatment. The black box is the section of the time during which the pods experienced heavy rainfall.....	33
Figure 3-9: Measured resistive strength to normal stress (penetrometer) for MICP treated surface sediments during the first series of Dellanera Beach tests.....	34
Figure 3-10: Photos of test pods at Dellanera Beach at week 3 of the experiment. From left to right: control plot, pH 9, bicarbonate.	35

Figure 3-11: Measured resistive strength to normal stress (penetrometer) for MICP treated surface sediments (i)-(iii) and untreated sediment during the second series of Dellanera Beach tests..... 36

Figure 4-1: Photo of geo-synthetic bag made of Mirafi S3200 material. Left panel: empty bag prior to filling. Right panel: bag with evenly distributed button drippers inserted into the geofabric surface..... 40

Figure 4-2: Slope Test Setup shown for the test involving rocks. The wire spool was used to increase the height (and therefore slope) of the rock matrix..... 42

Figure 4-3: Visual evidence of calcification in MICP-treated rock-sand matrix after complete slope failure of test (iii). Calcification is visible as an off-white color while remaining pockets of sodium bicarbonate deposits are bright white. 44

Figure 4-4: Measured slope angle versus total number of failed rocks for all runs of tests (i), (ii), and (iii). Values for duplicates in each test are indicated by respective lighter and darker shade symbols. 45

Figure 5-1: Top panel: Measured pressure (raw and 10-min average) in the surf zone near Dellanera RV park on Galveston Island. Bottom panel: Cross-shore (blue) and alongshore (red) velocity components measured at the same location. The total duration was about 7 days including landfall of Hurricane Laura. 47

Figure 5-2: Left panels: 100-second excerpt of pressure and velocity time series during storm impact..... 48

Figure 5-3: Top panel: Hourly wave height (significant and maximum) during the 7-day deployment..... 50

Figure 5-4: Google Earth image of the beach near Dellanera RV Park including place marks of individual sampling locations for two sediment sampling campaigns. 51

Figure 5-5: Average grain size distribution for Campaign 1. 52

Figure 5-6: Average grain size distribution for Campaign 2. 52

List of Tables

Table 2-1: Summary of initial laboratory test variations and results..... 14

Table 3-1: Field experiment timelines. 31

Table 3-2: Photos of MICP treated sediment surface comparing glucose and fructose effects..... 32

Acknowledgements

This work was supported by the U. S. Army Corps of Engineers – Galveston District (SWG) with funding provided under Cooperative Ecosystem Studies Unit (CESU) agreement No. W912HZ-17-2-0023 to Texas A&M Engineering Experiment Station (TEES). The authors would like to thank Patrick Kerr (USACE SWG), Coraggio Maglio (USACE SWG), Emily Perron (USACE SWG), Sheryl Rozier (Galveston Park Board of Trustees), Kimberly Danesi (Galveston Park Board of Trustees), and Larry Wise (Baird & Associates) for their support, guidance, and feedback throughout the course of the study.

1 Introduction

This report details TAMU/TEES activities and findings related to the project entitled: “Microbially-Induced Calcium Carbonate Precipitation (MICP) Supporting Nearshore Dellanera Reef Design for Galveston Island”. This project is a task under the overall Coastal Ecosystem Studies Unit (CESU) agreement No. W912HZ-17-2-0023 between the U.S. Army Corps of Engineers (USACE) and Texas A&M Engineering Experiment Station (TEES) entitled “In-Situ Measurements of Physical Forces and Biological Parameters in Coastal and Estuarine Systems, Galveston District”. The TAMU/TEES tasks that are part of this project include laboratory and field testing to optimize the MICP process and evaluate its feasibility for use in coastal erosion and flood risk mitigation measures and structures. These measures may include beach and dune sediment stabilization, rock revetments and rubble mounds combined with MICP treated sand, as well as submerged wave control structures such as reefs and sills which are a focus of the present study.

1.1 Background

The coastline of Galveston Island near the western end of the Galveston seawall features a prominent erosional hotspot. The beach at that location in front of Dellanera RV Park experiences the highest erosion rates (-8 ft per year) of Galveston Island. Due to the proximity to Highway 3005, the main evacuation route for Galveston in the event of severely inclement weather, the beach is a crucial line of defense. Without proper dune height and berm width, storm surge and wave attack could breach the highway and prevent evacuation, trapping residents on the island. Various nourishment efforts at this site have proven to provide only limited and temporary protection due to the highly erosive nature of the location and thus additional mitigation measures are being investigated.

Coastal protection schemes call for innovative solutions that should work with nature to achieve optimal outputs and multi-functionality. One solution to wave attack and erosion problems is the design and monitoring of submerged wave and sediment-guidance structures, such as submerged nearshore artificial reefs or sandbars. The use of microbially-induced calcium carbonate precipitation (MICP) to create environmental-friendly durable submerged reefs is a promising

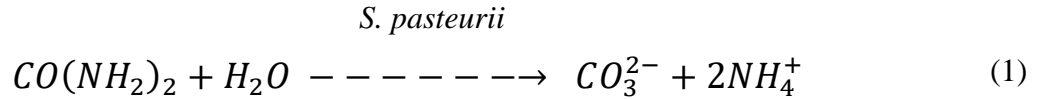
approach for this purpose requiring further field and laboratory testing (e.g., Seifan and Berenjian, 2019) with specific application to the Galveston environment.

Part of the TAMU/TEES scope for this project is to investigate the feasibility of MICP processes for submerged reef creation in the Galveston nearshore environment. This research task is part of a larger Planning Assistance to States (PAS) project conducted by the USACE in collaboration with the Galveston Park Board of Trustees, consulting firm Baird, and the Texas General Land Office (GLO). The PAS project includes numerical modeling and design of a submerged nearshore multipurpose breakwater in the shallow offshore waters near the west end of the Galveston seawall. The goal is to dissipate incoming wave energy and rotate incoming wave crests leading to salient formation in the lee of the reef. The overall study investigates long term geomorphic evolution (USACE numerical modeling efforts) and design of the structure including materials, structural stability, and construction methodology (USACE and Baird). The use of MICP is an option that would allow naturally occurring sediment to be used for complete reef construction (e.g., bare sand or inside geofabric bags), or as cement replacement between individual armor units or rocks. The following section provides a brief review of some literature on MICP and its use in enhancing the physical resistance of sediment against abrasion, compaction, and erosion.

1.2 Literature review

Microbially-Induced Calcium Carbonate Precipitation (MICP) is an innovative approach to limit erosion by using naturally occurring microbes (Gebru et al., 2021). The process can occur naturally under the right conditions but can also be induced artificially by creating optimal conditions for the microbes to form calcium carbonate precipitation. The process binds sand grains together through calcite formation at particle-particle contacts (Montoya, 2012), effectively creating a sediment grain matrix with increased resistivity against physical forces compared to loose granular sand. Montoya (2012) showed that the use of the urease producing bacteria *Sporosarcina pasteurii* (*S. pasteurii*) increases the MICP process when applied in local environments. Calcium carbonate production is commonly achieved by urea hydrolysis, which also produces ammonium and bicarbonate ions (Fujita et al, 2008; and Equation 1). The binding of sand grains can be seen using microscopic imaging, but visible calcification can sometimes be identified as a white layer on the surface of the sediment being tested. MICP can increase the strength and stiffness of sediment but

also reduce void space between grains. The biochemical process occurring during *S. pasteurii* induced calcite precipitation can be expressed as



where *S. pasteurii* acts on $CO(NH_2)_2$ (urea) and H_2O (water) to produce CO_3^{2-} (carbonate) and NH_4^+ (ammonium) and Ca^{2+} (calcium). The Ca^{2+} then chemically precipitates with CO_3^{2-} as $CaCO_3$ (calcium carbonate).

The effectiveness of MICP treatment has been assessed mainly via changes to soil shear strength and soil stiffness but other parameters including particle size, shear wave velocity, porosity, permeability, and calcium carbonate content can be assessed to determine its effectiveness (Geburu et al., 2021; Landa-Marbán et al., 2021; Nafisi and Montoya, 2018). The shape of individual sediment particles as well as the grain size distribution can affect the level of cementation even if the samples display equivalent shear wave velocities (Nafisi et al, 2018). Multiple studies have shown that MICP improves the strength and stiffness of unsaturated sand. This bio-cementation could provide a more environmentally friendly replacement for traditional coastal protection structures such as seawalls and revetment type structures (Shanahan and Montoya, 2016). Sand dunes are a natural coastal defense structure that are commonly the first line of defense when a storm occurs. Strengthening these dunes would allow for stronger defenses against storms. Shanahan and Montoya (2016) investigated the impact that MICP has on sand dunes when they are subjected to wave action. The MICP solutions that were used in this study contained yeast extract media, calcium chloride, and urea solution. The yeast extract media was inoculated with *S. pasteurii* stock culture. Sand was placed in a 2-ft by 2-ft box that was placed at an initial angle of 15° as that was representative of sand dune slopes in the area where the study was conducted. Results showed that after wave testing the eroded cross-sectional area of moderately cemented sand was 1.6 in^2 while the uncemented sand experienced an eroded area of 3 in^2 (almost double). Thus, microbially induced calcium carbonate precipitation (MICP) could be used to reduce wave-induced erosion when applied to sand dunes (Shanahan and Montoya, 2016).

Scour mitigation can be achieved by enhancing the ability of the bed material to resist flow-induced shear stresses or by reducing the impact of scouring agents. However, many approaches are expensive and time consuming (Chiew, 1992). MICP can provide a cost-effective alternative that utilizes natural microbes in the nearby environment. Chiew (1992) tested the strength of MICP-treated sediment using a submerged impinging jet system. This system induces shear stress onto the surface of the material by submerged impinging jet flow (Montoya et al., 2018). As the flow rate increases, the depth of scour also increases. While the sample was being prepared, three different shear wave velocities were used to determine cementation levels: 400 m/s for lightly cemented, 700 m/s for moderately cemented, and 1200 m/s for heavily cemented. The shear wave velocities acted as a marker for different levels of cementation and were determined by dividing the length of the 10-V sinusoidal wave, with a frequency of 10 kHz, by the time it took for the transmitted signal to be received by the oscilloscope (Montoya et al., 2018). To achieve the designated shear wave velocity, the samples were injected with the MICP solution and drained at 40 mL/min until the desired shear wave velocity was reached, maintaining a saturated condition. The injections allowed Montoya et al. (2018) to investigate how the urease and bacteria were affecting the sand. Results showed that precipitated calcium carbonate accounted for 1%, 2.5%, and 5% of the total mass for the lightly, moderately, and heavily cemented samples, respectively. Erosion testing showed that the untreated and lightly cemented sands had similar erosion rates to uncemented sands (Montoya et al., 2018). However, the moderately and highly cemented samples showed erosion rates like those for plastic silt and clay. Critical shear stress and erodibility coefficients increased by 1 to 4 orders of magnitude based on cementation levels.

MICP has been investigated by various researchers for different applications including ground stabilization against liquefaction (e.g., Feng and Montoya, 2017) and coastal sand hardening (e.g., Ghasemi and Montoya, 2020). MICP testing has been performed in many laboratory settings but far less in field applications. Gomez et al. (2015) conducted an MICP field calcification test up to a depth of 30 cm in Saskatchewan, Canada. Four test plots measuring 2.4 m by 4.9 m were established with three receiving varying MICP concentrations and one plot receiving only water in various volumes. The plots were treated five times with an interval of 4-day cycles where day 1 included bacterial treatment and the other three days included nutrient treatment. Both treatment solutions were the same except for the added *S. pasteurii*, which was not included in the nutrient treatment. A volume of 376 L at a flow rate of 19 L/min was added to each of the test plots daily

and samples were tested daily using a dynamic cone penetrometer. The results showed that the lowest concentration of treatment had the highest calcification both on the surface and at 10 cm depth. Ultimately, this study showed that lower concentrations of MICP can be more effective under certain conditions and that MICP could prove to be a practical tool for erosion reduction.

Several biological processes have been shown to play a role in MICP formation (Mori et al., 2021; Mondal et al., 2019; Kim et al., 2018). Under anaerobic or hypoxic conditions, microbes tend to produce a variety of weak acids such as lactate, propionate, acetate and formate that help them re-oxidize the reducing power ($\text{NAPH} + \text{H}^+$) produced by catabolism of carbohydrate, proteins or lipids (Verduyn et al., 1990; Eiteman et al., 2015). These acids increase the alkalinity of the solution they are produced in thereby inducing precipitation of carbonate along with calcium to form calcium carbonate. On the other hand, research has shown that oxygen availability is crucial for MICP formation (Li et al., 2021). Most of the researchers studying MICP have focused on urea hydrolysis by urease producing bacteria as the key process (Ferris, 2003; Fujita et al., 2000; Warren et al., 2001; van Passen, 2009), primarily because urea hydrolysis is the first process associated with MICP (Ehrlich, 1996). However, it is suggested that urea hydrolysis might only play a fractional role in MICP primarily due to the lower abundance of urea (van Paassen, 2009). Although, urea hydrolysis has been proven to be an efficient way to manually induce MICP, the lack of research on other biological processes such as bacterial weak acid production may indicate that the maximum efficiency of MICP still remains to be realized. Simple factors such as growth media for *S. pasteurii* and optimal pH for the MICP process are still being determined (Omoriegbe et al., 2019; Kim et al., 2018). Using naturally occurring microbial community may have some advantages over the traditional use of urease producing *S. pasteurii*. The use of natural microbial community will have no unintended consequences on the biological structure of the MICP site and is therefore environmentally safer over introducing a foreign strain of bacteria (i.e., *S. pasteurii*) that can potentially overgrow the naturally occurring microbial population (Marin et al., 2021; Rajasekar et al., 2021). This, however, is not an issue if *S. pasteurii* is used in a saltwater environment since these bacteria are freshwater microbes and cannot survive in a saltwater environment. Another advantage of the use of natural microbial community is the fact that these do not solely rely on urease activity to induce MICP. Rather, a complex combination of weak acid fermentation is induced. This significantly reduces levels of toxic by-products such as ammonia compared to the traditional process of using *S. pasteurii*. Using natural microbial community over

the traditional process may increase the potential of MICP as an environmentally safe process, however, levels of toxic byproducts using *S. pasteurii* are thought to be relatively low for the scope of this project and not harmful to the environment.

1.3 Motivation and objectives

The intent of the overarching PAS project is to include natural and nature-based features (NNBF) and EWN principles to effectively and sustainably deliver economic, environmental and social benefits to this submerged reef project. Investigating the implications of using MICP processes to aid in the creation of submerged reefs that can help mitigate shoreline erosion is the principal focus of the TAMU/TEES research task. The three main research objectives are:

- 1) the determination of the optimal conditions and parameters to achieve maximum efficiency in the MICP process using sand from the project location;
- 2) the assessment of best practices for use of MICP enhanced sand in coastal erosion and flood risk reduction measures such as submerged reef design and construction;
- 3) the collection and analysis of select hydrodynamic and sediment data at the field site to supplement the design process.

Objective 1 is accomplished through laboratory testing of various strategies to induce MICP processes. Aside from adding calcium chloride (CaCl_2) solution to the sand, this includes comparing the traditionally used *S. pasteurii* (formerly known as *Bacillus pasteurii*) over naturally occurring microbial communities at the project site and determining the significance of urease activity on MICP. Both aerobic and anaerobic conditions are tested as well as the addition of glucose to enhance the MICP process. In addition, different sources of organic carbon (glucose vs fructose), growth media (marine broth vs yeast extract), pH (5, 6, 7 and 9), and lastly impact of additional supply of carbonate ions (in the form of sodium bicarbonate) are assessed. Physical, biological, and chemical parameters of the MICP enhanced sand are measured and analyzed to identify the optimal configuration.

Objective 2 is accomplished via testing the optimal MICP configuration in the field. In-situ use of MICP to stabilize sand on the beach near the Dellanera RV park on Galveston Island is investigated. Both open surface and geofabric enclosed MICP options are tested to assess construction and

design practices for MICP submerged reefs. Further laboratory testing on the stability of rock slopes with and without the addition of MICP enhanced sand is carried out to address the potential use of MICP to improve common coastal revetment structure performance.

Objective 3 is accomplished through the deployment of an acoustic Doppler velocimeter (ADV) and a pressure transducer (PT) in the surf zone near the project site over a period of several days capturing calm and stormy conditions. In addition, several grab samples of the surface sand near the project site are collected and analyzed for sediment characteristics including grain size distribution.

2 Laboratory Experiments

A variety of laboratory experiments were conducted to optimize the MICP process. Setup, methods, and results from the most relevant experimental efforts are summarized in this chapter to complement items that had already been presented in the midterm report for this project.

2.1 Development of test protocols

Several laboratory experiments were performed to determine the optimal setup, parameters, and solutions for testing MICP formation (summarized in Table 2-1). For example, 50-mL plastic falcon tubes were used initially, but later upgraded to a syringe system (Figure 2-1) to allow for better circulation of the MICP-inducing solutions. The MICP process is induced by subjecting sediment to two different solutions. Solution S1 (bacterial mixture) introduces the microbes while solution S2 (cementation mixture) introduces the components needed for the microbe population to grow and produce cementation.

Parameters tested included aerobic and anaerobic conditions, layering and use of natural seawater or pure culture of *S. pasteurii* (Table 2-1). Several variations in MICP solutions were tested for optimal MICP formation, which includes the use of marine broth (a commercially available growth medium for cultivating marine bacteria) with and without urea for S1 and addition of glucose or fructose (Table 2-1). These experiments suggested that a syringe setup, under aerobic condition and a layering procedure of sand with *S. pasteurii* in marine broth containing urea (S1) and calcium chloride, urea, and fructose (S2) led to the strongest MICP formation among the tested options. Continued testing and fine-tuning may lead to further strengthening of the MICP process.

Table 2-1: Summary of initial laboratory test variations and results.

#	Test Composition	Structure* (Qualitative observation)	Relative Strength (Qualitative observation)	Penetrometer Reading** (kg/cm ² or tons/ft ²)
1	SW + Aerobic + CaCl ₂	Yes	Weak	Fell apart
2	SW + Aerobic + CaCl ₂ + Urea	Yes	Medium	Fell apart
3	SW + Anaerobic + CaCl ₂	No	N/A	N/A
4	SW + Anaerobic + CaCl ₂ + Urea	No	N/A	N/A
5	SW + Aerobic + CaCl ₂ + Urea + Glucose	Yes	Strong	Fell apart
6	(SW + MB) + Aerobic + CaCl ₂ + Urea	Yes	Medium	Fell apart
7	(SW + MB) + Aerobic + CaCl ₂ + Urea + Glucose	Yes	Strong	1.0
8	BP + Aerobic + CaCl ₂ + Urea	Yes	Strong	1.5 (crumbling bottom)
9	(SW + Urea + MB) + CaCl ₂ + Urea	Yes	Weak	Fell apart
10	(SW + Urea + MB) + CaCl ₂ + Urea + Layering	Yes	Weak	Fell apart
11	BP + Aerobic + CaCl ₂ + Urea + Layering	Yes	Strong	1.5
12	(SW + Urea + MB) + CaCl ₂ + Urea + Glucose + Layering	Yes	Weak	Fell apart
13	BP + Aerobic + CaCl ₂ + Urea + Glucose + Layering	Yes	Strong	>4.0 (exceeded scale)

* Qualitative observations include a binary classification of calcified structure formation. Tests labeled “yes” formed a sediment column. Tests labeled “no” remained granular.

** Resistive strength of the samples to normal stress were quantified using a pocket penetrometer.



Figure 2-1: Photo of syringe test setup exploring an alternate layering approach.

Another set of laboratory experiments was conducted with an alternative experimental setup adapted from Zhao et al. (2014). Cylindrical mesh wiring was formed to fit the mold used for the standard unconfined compression testing and secured using zip ties. Cheesecloth was attached on one end of the wire cylinder to act as a filter (Figure 2-2). Autoclaved sand from Dellanera Beach was used to fill three of the wire molds and three molds were filled with natural sand from the same location. The cylinders were then wrapped in cheesecloth including the top to minimize the loss of sediment during the experiment. The molds were then placed into an 18 L storage container and covered in a solution combining S1 and S2 (1.5M CaCl_2 + 1M urea + 18 g/L fructose) and exponential phase culture of *S. pasteurii*). An amount of 2500 mL of each solution was added to the container to cover the cylinders. A pump helped keep the container oxygenated. The container was then closed, and the cylinders were incubated in the container for seven days. After this duration the molds were removed from the containers followed by curing for seven days. After the columns had cured for seven days, MICP sediment columns stable enough were subjected to unconfined compression testing. In this experiment the cylinders were submerged in MICP solution compared to prior flow-through setups to assess any differences in MICP strength and occurrence between the two different treatment options. Results showed that the MICP process was more effective throughout the columns containing autoclaved sand. However, further experimentation is

required to confirm these observations for a larger variety of sediment and MICP solution setups. In particular, the comparison to the syringe tests is not straightforward as further optimization of the submerged test setup is needed for an apples-to-apples comparison. Some of the issues here relate to optimizing the fluid replacement rate and the issue of mixing autoclaved versus non-autoclaved sand. Future testing is anticipated to fill these knowledge gaps.



Figure 2-2: Experimental setup of cylindrical mesh molds submerged in MICP solution. Molds were created from wire mesh and were filled with autoclaved and natural sand from Dellanera Beach.

2.2 Methods

After optimization of the experimental procedures further laboratory experiments were performed to optimize the growth medium for *S. pasteurii* in terms of performance and cost. Yeast extract at three different concentrations (10, 20 and 30 g/L) along with 1 g/L of glucose and 2 g/L of urea was tested against the traditional marine broth medium in triplicates. Hourly growth of *S. pasteurii* was monitored by measuring the optical density at 600 nm using a UV-Visible Spectrophotometer (RF-5301PC; Shimadzu, Houston, TX, USA).

The next set of laboratory experiments was conducted to measure the extent of calcification using yeast extract as the growth medium at a concentration of 20 mg/L for *S. pasteurii*. Both growth and calcification were measured simultaneously at 0, 1, 2, 4, and 24 hours past the time of mixing S1 (*S. pasteurii* culture) and S2 (fructose corn syrup + CaCl₂ + urea). Growth was measured by monitoring the optical density of the solution as described above. Calcification was measured by

centrifuging two parallel 10-mL samples from each measuring point in time at 3000 rpm for 15 minutes. After the samples underwent centrifuging, they were separated into a liquid and a solid fraction. The solid fraction settled in the bottom of the Falcon tube. The liquid is referred to as supernatant while the solid fraction that settled is referred to as a pellet. The pellets were then resuspended in 1 mL of distilled water and washed twice by centrifuging at 10,000 g for 5 minutes. One of the two pellets was then resuspended in de-ionized (DI) water at pH 9, while the other was resuspended in DI water at pH 6.5. The samples were then transferred into pre-weighed microcentrifuge tubes and centrifuged again at 10,000 g for 5 minutes. Once the supernatant (the volume of liquid above the pellet following centrifugation) was discarded, the pellets were dried overnight in an oven at 60°C and weighed again. The difference in weight of the microcentrifuge tubes is an indicator of calcification.

The effect of individual S2 components was determined via another laboratory experiment. The experiment included three treatments, wherein the individual components of S2 were not included. Therefore, the three different S2 options were the control (fructose + CaCl₂ + urea), CaCl₂ + fructose, and urea + fructose. Growth was measured hourly immediately after the mixing of S1 (*S. pasteurii* culture) and the different S2 options. Growth was measured by monitoring the optical density of the solution as described above.

2.3 Results

Comparison of growth of *S. pasteurii* under different concentrations of yeast extract revealed significantly higher growth in all the concentrations of yeast extract compared to marine broth ($p < 0.0001$, one-way ANOVA) as indicated in Figure 2-3. Further analysis revealed concentration-dependent growth in yeast extract with increased concentrations resulting in enhanced growth after 8 hours of incubation. However, at the 6-hour mark the growth rates for the different concentrations of yeast extract were only slightly different ($p < 0.0117$, one-way ANOVA), which underscores the importance of incubating the *S. pasteurii* culture beyond the 6-hour mark.

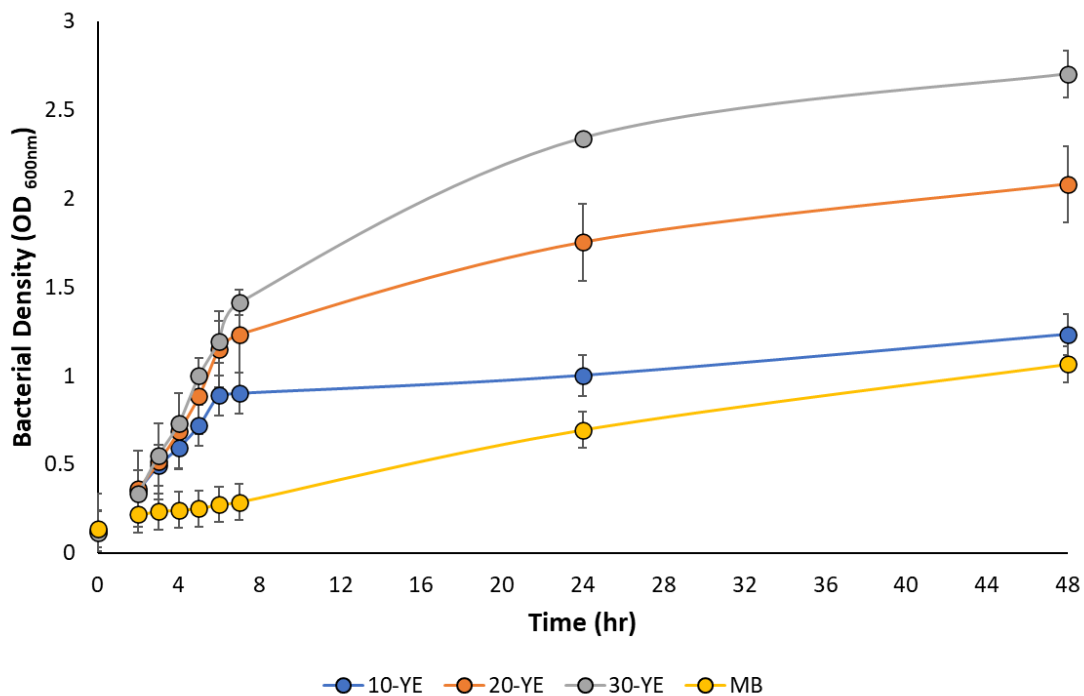


Figure 2-3: Growth of *S. pasteurii* in marine broth (MB) and different concentrations of yeast extract (YE) with 1% glucose.

The extent of calcification was then measured in the identified optimal growth medium (yeast extract; 20 mg/L). The optimum yeast extract concentration was determined as the concentration with the greatest potential for further growth (i.e., the largest slope leading up to the 48-hour mark) with the second criteria being cost. The results indicated saturation in calcification and growth after two and four hours, respectively (Figure 2-4). The discrepancy between the observed initial growth in the presence (Figure 2-4) and absence (Figure 2-3) of S2 components at 20 mg/L of yeast extract is primarily due to the slight difference (one generation) in the bacterial concentration in the inoculum (starter culture) used to begin the experiment. The discrepancy between the observed growth trend in the presence (Figure 2-4) and absence (Figure 2-3) of S2 components at 20 mg/L of yeast extract suggests that one or more components of S2 might be inhibiting growth and therefore calcification.

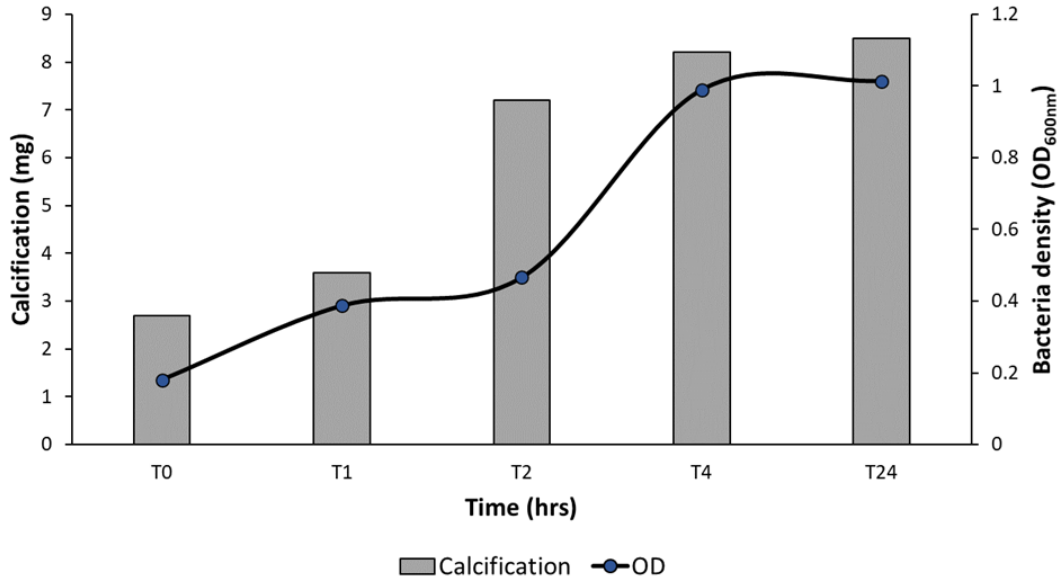


Figure 2-4: Calcification and growth in 20 mg/L yeast extract (S1).

The next set of experiments was conducted to test the effects of different components of S2 on the growth of *S. pasteurii*. The results indicated that S2 solution without urea (but with CaCl₂ + fructose) resulted in significantly higher growth ($p < 0.0039$, One-way ANOVA) based on measured optical density (OD). The control S2 and S2 including urea + fructose resulted in similar but lower growth ($p = 0.8117$, One-way ANOVA) over a period of 24 hours as shown in Figure 2-5.

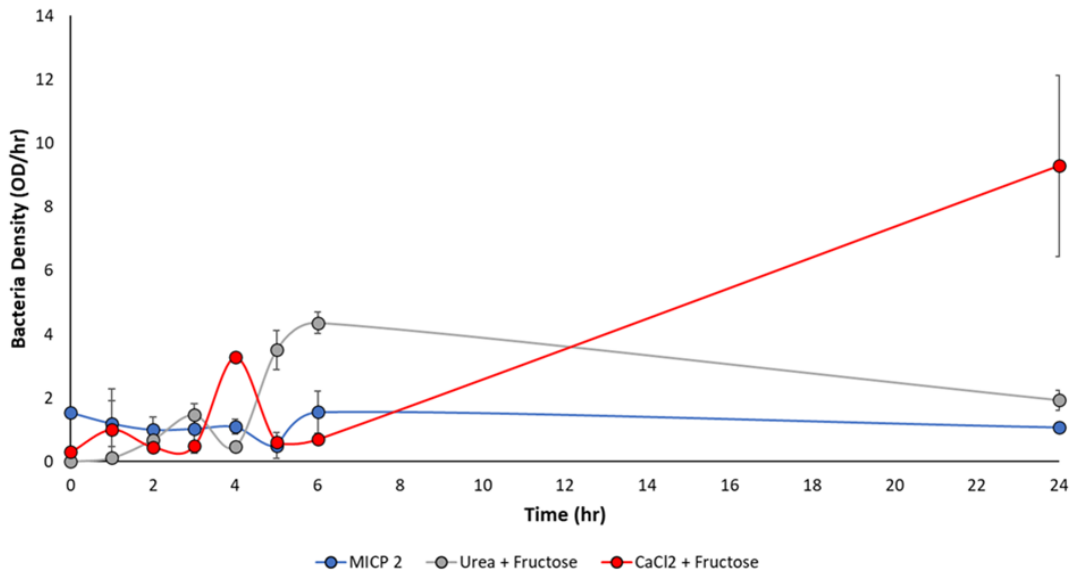


Figure 2-5: Growth of *S. pasteurii* using S1 combined with different S2 options.

Analysis of pH indicated that S2 without urea (CaCl_2 + fructose) resulted in near neutral pH after 2 hours of incubation. The pH in S2 without urea (CaCl_2 + fructose) were also significantly higher than the other two treatments ($p < 0.0001$, One-way ANOVA). However, the pH in control S2 remained acidic throughout the course of the experiment, whereas S2 including urea + fructose turned to acidic pH past the 4-hour mark as shown in Figure 2-6.

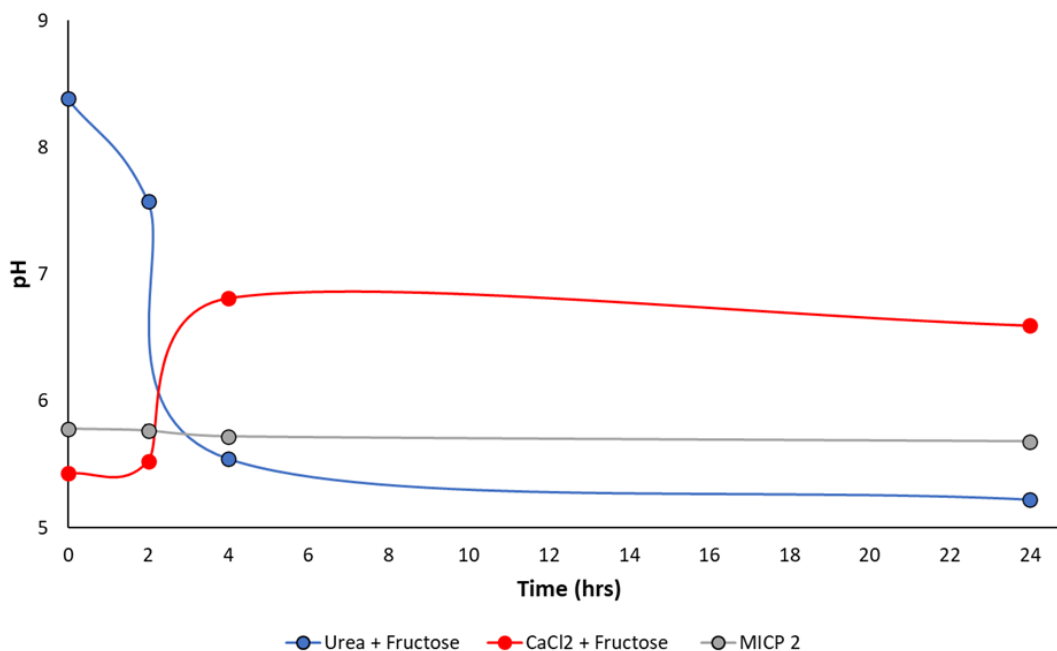


Figure 2-6: Growth medium pH value under S1 and different S2 options.

2.4 Discussion

To determine the optimal parameters for inducing calcification using the sand from Galveston beach, several parameters were tested as listed in Table 2-1. The first setup focusing on testing whether anaerobic conditions would favor calcification suggested better performance under aerobic conditions, similar to observations made by Jain et al. (2019). A study conducted by Sun et al. (2019) suggested that addition of glucose improved calcification. We therefore coupled glucose addition with prior incubation of seawater with marine broth to test whether the increase in bacterial density can further boost the MICP process. The results from this project confirmed the Sun et al. (2019) study and showed improved strength with glucose addition, which was further enhanced by incubation with marine broth. However, since the sand columns formed using the

above setups were still relatively weak, the next test setups used the traditional bacterial strain *S. pasteurii* (Omoregei et al., 2017). Results indicate that calcification occurred only on the surface, suggesting the need for improvements in solution delivery for more uniform calcification. This led to testing the effect of the layering process described above on promoting uniform calcification in the sand columns. These test results indicated improved calcification upon layering, which further benefited from addition of glucose. However, the use of indigenous bacteria from seawater formed relatively weaker sand columns compared to *S. pasteurii*. This observation contrasted with the Baidee et al. (2019) study, wherein indigenous bacteria resulted in MICP columns with similar strength. The observed discrepancy in observation with the Baidee et al. (2019) study could be due to differences in soil properties.

Considering the improved results of strength of the sand column, the next choice was the combination of *S. pasteurii* with glucose addition and layering for preliminary field tests on the TAMUG campus (see Chapter 3). Multiple field tests have been conducted using the bacterium *S. pasteurii* in the past (Cuthbert et al., 2013; Phillips et al., 2016; Phillips et al., 2018) with no concerns associated with environmental safety, suggesting the application of this bacterium at the proposed field site is safe. In addition, the concentrations of CaCl_2 and urea utilized in this study are relatively low to have any negative impact on an environmental scale through discharge of MICP-inducing solutions. However, challenges remain regarding the application of this process on a larger scale. For example, marine broth used to grow *S. pasteurii* is expensive and the addition of pure glucose will further increase the cost of this process. This can be addressed by use of a simpler growth medium containing yeast extract or molasses for cultivating *S. pasteurii* and use of fructose corn syrup rather than pure glucose. Although, the use of indigenous bacteria resulted in relatively weaker sand columns, a sand column with increased strength (penetrometer reading of 1 kg/cm^2) formed in preliminary laboratory test #7 (Table 2-1). As all the preliminary setups were performed at various times/seasons, wherein the natural bacterial community might have varied, our observations highlight the potential for improvement through isolation of bacteria from different seasons throughout the year and further testing for improved MICP in the future.

Marine broth has been traditionally used as a choice of growth medium for *S. pasteurii* (Horiike et al., 2017; Venda Oliveira et al., 2015; Park et al., 2012). Comparison of different concentrations of yeast extract with 1% glucose as an alternative growth medium to the traditional use of marine broth resulted in significantly higher growth of *S. pasteurii* for all tested concentrations of yeast

extract. Given the 10% cheaper cost of yeast extract compared to marine broth and 2.5-fold higher growth of *S. pasteurii* (both at 20 g/L), the former is an optimal choice of growth medium both in terms of biomass productivity and cost. The variations in growth obtained with different concentrations of yeast extract have implications for the time needed to prepare the *S. pasteurii* solution for MICP preparation. For instance, similar growth between 20 and 30 g/L of yeast extract within the first 6-8 hours means 20 g/L is the more cost-effective concentration if the time available to prepare the *S. pasteurii* solution is equal to or around 8 hours. A yeast extract concentration of 30 g/L is the optimal concentration of growth medium if more than 24 hours are available for the preparation of the *S. pasteurii* solution for MICP and cost is not a major factor.

A comparison of growth patterns observed in Figure 2-5 and Figure 2-6 indicated relatively lower growth in the presence of the control S2, suggesting one of the components of the control S2 might be inhibiting the growth, therefore limiting the maximum amount of calcification that can be ideally obtained. The higher growth observed in the absence of urea in a modified S2 combined with the neutral pH suggested the presence of urea could be causing the pH of the medium to turn acidic, presumably through the generation of CO₂ from the activity of urease on urea (Yamauchi et al., 2019). Moreover, a pH level below 8 has been shown to negatively impact calcification (Ries, 2011). Additional sets of laboratory experiments are required in the future to test the impacts of acidity on the calcification process and determine the optimal pH for MICP.

3 Field Testing

Preliminary field experiments were carried out using test pods on the TAMUG campus and the main field experiments were conducted on the open Galveston beach at Dellanera RV park. An overview of the various setups, testing methods, and results is given in this chapter.

3.1 Setups and locations

Test pods consisting of wood frame enclosures were placed at various field locations to separate the MICP-treated sediment from the surrounding sediment. They were approximately 2 x 2 x 2 feet in dimension with half of their height extending below grade. Figure 3-1 shows two examples of field pods in use, one with sediment filled to the top and one where the sediment surface inside the pod is at the same level as the surrounding sediment.

The pressure-treated wood panels and posts making up the pods fulfilled several functions. Apart from creating a confined test bed for MICP treatment, they also prevented direct erosion of sediment from wave runup at beach locations. Furthermore, the pods could be outfitted with lids to protect the MICP process from the elements and filter cloth could be added at the bottom of the pods to limit efflux of microbes beyond the pod depth.



Figure 3-1: Photos of test pods with sediment filled to the top (left) and at grade (right).

MICP solutions were applied to the test pods via surficial spraying using two different systems. The first system consisted of a small pump, hose, and micro sprayer nozzle optimized for delivery of the desired flowrate and even distribution of the MICP-inducing solutions. The 158-gph

submersible pump (Model: EcoPlus Eco 185) has an oil-free magnetic drive with a rare earth rotor magnet. The ceramic shaft impeller enables this pump to be used in freshwater or saltwater. This method required a power source to be used in the field. The second setup employed manual pump action graduated containers (7.5 L, 2 gallons) with micro sprayer nozzles. These are typically used in lawn and garden applications and do not require an additional power source. Figure 3-2 shows both systems.



Figure 3-2: Photos of two different MICP solution delivery systems for field experiments. The left panel shows the pump, hose, and nozzle setup. The right panel displays the graduated manual sprayer containers being filled with MICP solution prior to a field test.

For preliminary field experiments conducted on the TAMUG campus, the setup was adapted from Salifu et al. (2016) with amendments and processes based on findings from already completed laboratory experiments. Three pods were placed in sandy ground and the top half of the first pod was filled with local Galveston beach sand through a process involving alternate layering. The first layer consisted of approximately 18 kg of sand poured and uniformly distributed inside the frame, followed by the addition of S1 (1M CaCl_2 + 1M urea + 1g glucose/L) using the pump, hose, and nozzle system. The second layer consisted of sand (~18 kg) followed by the addition of S2 (exponentially phased culture of *S. pasteurii*) using the same spraying system as for the application of S1. The layering process was repeated until the top 30 cm of the frame were filled, resulting in approximately five layers, three of them including S1 and the remaining ones including S2. The first experiment that was conducted on the TAMUG campus was conducted before lab experiments showed that urea had a negative impact on the MICP process. Based on literature, S1 in this

experiment included urea. The two additional pods tested on the TAMUG campus were filled in the same manner except that the bottom half of the pod was filled with Galveston sand. The pod was filled to a level that was even with the soil surface outside of the pod.

The main field experiments were carried out on the subaerial beach near the end of the Galveston seawall between the mean high tide line and the dune foot. This location was chosen due to its proximity to the envisioned submerged reef site offshore of the Dellanera RV park and ease of access. The MICP process works best under relatively dry conditions which is why the test pods were placed on the part of the beach that is not frequently inundated with water.

Figure 3-3 shows an overview map of the two field site locations as indicated by the two arrows. A closer view of the Dellanera field test site including mean low and high tide lines in relation to the test pod locations is given in Figure 3-4. A cross-sectional view depicting representative beach profiles near the field pod locations on Galveston Island is given in Figure 3-5 based on profile measurements conducted after Hurricane Harvey in 2017. The yellow profile is located near the western end of the Dellanera RV park, and the gray profile is located close to field pod site just west of the end of the Galveston seawall. The mean low and mean high tide lines are shown by red and blue horizontal lines, respectively. Elevations are based on NAVD88.

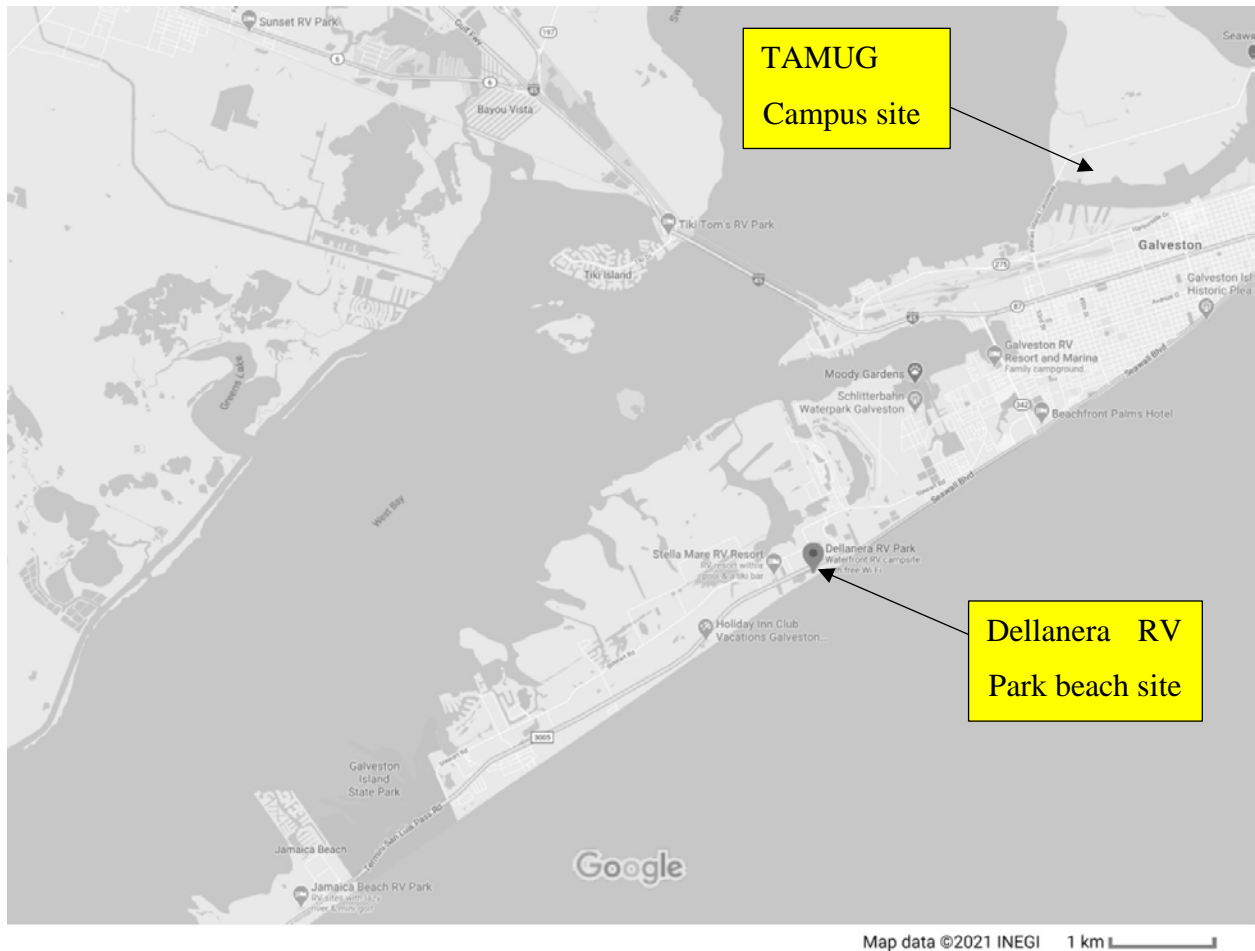


Figure 3-3: Overview map showing field experiment locations on the TAMUG campus and on the beach at the end of the Galveston seawall near Dellanera RV park.

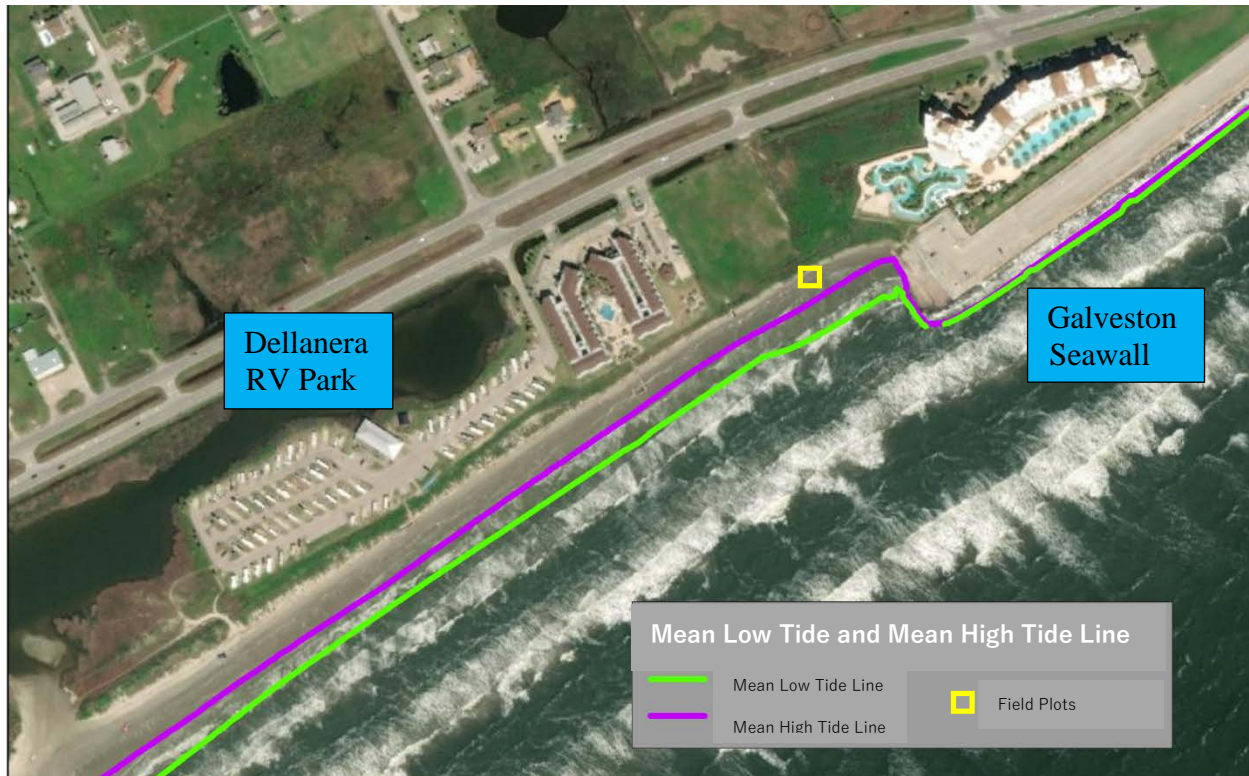


Figure 3-4: Planview of project area and field pod locations (yellow square) near Dellanera RV Park on Galveston Island just west of the western end of the seawall. The mean low and mean high tide lines in the vicinity of the project site are shown by green and magenta lines, respectively.

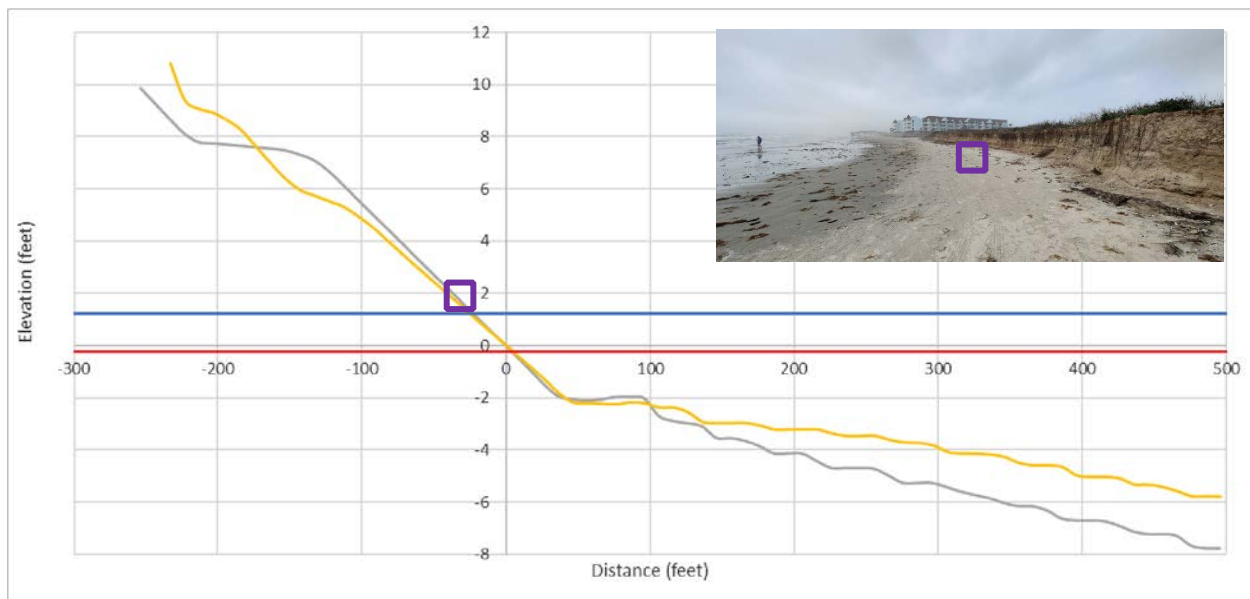


Figure 3-5: Cross-shore profiles at the project site and corresponding photo (looking west) of the beach and dune scarp. Field pod site locations are indicated by the purple squares.

The General Land Office (GLO), City of Galveston, and the Galveston Park Board of Trustees did not require a formal permit to conduct the planned field experiments on the beach at Dellanera RV Park as was determined through discussions with each entity. All three entities, however, were kept informed regarding test schedule and images from the field setup. Under Section 10 of the Rivers and Harbors Act the USACE regulates the construction of any structure in or over any navigable waters of the United States. A regulatory permit for the field work near the mean high tide line was submitted to the USACE SWG regulatory branch for approval. On March 30, 2021, the decision letter that no permit is required was issued. This decision was also reached in consultation with the Clearlake office of the National Fish and Wildlife Services indicating that there are no concerns regarding the project considering the Endangered Species Act (ESA).

Signage was included with the field pods to deter the public from interfering with the field setup and MICP process. A simple explanation of the experiment was included to inform the public of the study taking place.

3.2 Methods

Preliminary TAMUG Campus Tests

For the TAMUG campus field tests surficial spraying of the sand surface was conducted using the pump, hose, and sprayer system described in Section 3.1. Both MICP-inducing solutions (S1 and S2) were applied three times a day for six days at a rate of 4 mL/s for 120 s, respectively. The top of the test plot remained exposed to the environment throughout the entire experiment period to allow for the sun to contribute to reducing moisture within the sand column (Figure 3-6). Both raised and at-grade test setups were used. A variation of S2 using fructose instead of glucose was also tested. The modified S2 formula was 1M CaCl₂ + 1M urea + 18 g/L fructose. MICP-inducing solutions were applied three times a day for six days at the same rate of 4 mL/s for 120 s. At the end of each day, a tarp was used to cover the test pods to limit moisture entering the pod as well as prevent any other interference with the ongoing test.



Figure 3-6: Photos of raised-bed pod setups on the TAMUG campus. Left: Day 1 also showing the solution application system. Right: Field plot on day 22 after initial setup.

Dellanera Beach Tests

Two series of beach tests with natural Galveston sand were conducted. A total of five pods were set up with sediment at grade with the surrounding surface sediment after the initial sand layering process was completed as explained in Section 3.1. The mixing process involved treating each layer of sand with 1 L of each respective MICP solution (S1 or S2, respectively). MICP solution S2 consisting of 1M CaCl₂ + 1M urea + 18 g/L fructose was used for the first test series. A 2.54-cm (1-in) thick filter fabric was attached to the bottom of the test plots to limit the amount of solution lost to the environment below the depth of the test pod. Measurements commenced after an incubation period of 14 days during which the MICP reaction and calcification was allowed to happen. Protective tarps were draped over the pods at night. In the first series of tests, two pods were set up.

For the second series (three pods) of beach tests, S1 remained the same (an exponential phase culture of *S. pasteurii* in a growth medium containing 20 mg/L of yeast extract), but the formula for S2 was altered to test the effects of elevated pH level and additional supply of carbonate ions in comparison to the control version of S2. For this test, the three different recipes for S2 were:

- (i) Control S2: 1M CaCl₂ + 1M urea + 18 g/L fructose
- (ii) Elevated pH: By adding sodium hydroxide solution to the control S2, pH was raised from 6.5 to 9.
- (iii) Bicarbonate and elevated pH: 0.5M sodium bicarbonate was added to the elevated pH S2.

Four pump-action spray containers were used to apply the MICP solutions to the sand surface inside three pods setup side-by-side (Figure 3-7). Latched lids made of plywood were used to cover the pods and to prevent excessive rainwater intrusion. A volume of 1 L of S1 was sprayed evenly on each of the test plots followed by 1 L of the respective S2 version (i) – (iii). This process was repeated three times a day over six days. Measurements began after an incubation period of 14 days to allow the MICP reaction and calcification process to occur. Table 3-1 shows the typical field experiment timeline. For series 2, penetrometer readings were taken in triplets once a week over a 5-week period (November 10 to December 9, 2021) to quantify the resistive strength of the samples to normal stress. Unlike the first field setup at the beach, readings were taken once weekly as the integrity of the pod was important to maintain. The weekly readings still allowed for meaningful results to be gained. A pocket penetrometer was used to apply normal pressure to different sections of the sand surface in each pod. Visual observations of the sand surface were also noted.



Figure 3-7: Photo of pod setup used in the second beach test series.

Table 3-1: Field experiment timelines.

	<i>S1 & S2 Application</i>	<i>Curation</i>	<i>Data Collection</i>
<i>General Timeline</i>	Days 1-6	2 weeks	Series 1: Every 2 days Series 2: Once per week over 5 weeks
<i>Series 1</i>	Jun. 21-26, 2021	Jun. 27 – Jul. 11, 2021	July 5-15, 2021
<i>Series 2</i>	Oct. 18-23, 2021	Oct. 24 – Nov. 7, 2021	Nov. 10 – Dec. 9, 2021

3.3 Results





TAMUG Campus Tests

Figure 3-6 showed a comparison between two field pods on the TAMUG campus at day 1 and day 22 after initiation, respectively. The raised above-grade setup of the treated sediment column was chosen to avoid any pooling surface water or ground water affecting the MICP process. In these initial test setups, no visual calcification and relatively poor stability was observed with the produced column falling easily even 21 days past the initial setup.

Further TAMUG campus field test comparing the use of fructose versus glucose as food for the microbes were conducted. Penetrometer readings were recorded starting on Day 12 of the experiment. Testing began on April 19, 2021 and continued until May 18, 2021. Once slight calcification began to appear on the sediment surface of the fructose pod, penetrometer readings were taken at locations with lighter coloring. Table 3-2 shows photos of the glucose and fructose pods on Day 2 of treatment. The sand was very moist from the treatment solutions and from the surrounding Galveston humidity. As the experiment progressed, visual indications of slight calcification were observed on the surface of the pod containing the fructose treatment with lighter spots scattered across the sand surface. This surface calcification was more concentrated toward the center of the sediment surface inside the pod. In the pod containing glucose, a small layer across the surface showed a slight increase in strength, however the strength decreased as algae and fungus began to grow creating a green layer across the surface of the sediment. The bottom row of Table 3-2 shows photos of the pods on Day 20 of the experiment, where the surface calcifications spots can be observed in the sediment treated with fructose. The sediment treated with the fructose S2

exhibited an overall increased resistance (up to 2.5 times) to normal stress compared to the treatment with glucose S2 (Figure 3-8). Resistance to normal stress was measured using a pocket penetrometer with each data point representing averages of four separate measurements within each pod, respectively. However, heavy rain on day 20 through day 23 caused water pooling in the test pods and saturated the sediment. This made data collection more difficult and caused a significant drop in the resistive strength of the surface sediment treated with fructose S2. The MICP process in the sediment treated with glucose S2 was less affected by the rainwater intrusion and continued with slight increases in resistance to normal stress application after only a slight dip during the onset of the wet conditions.

Table 3-2: Photos of MICP treated sediment surface comparing glucose and fructose effects.

Day	S2 with glucose	S2 with fructose
2		
20		

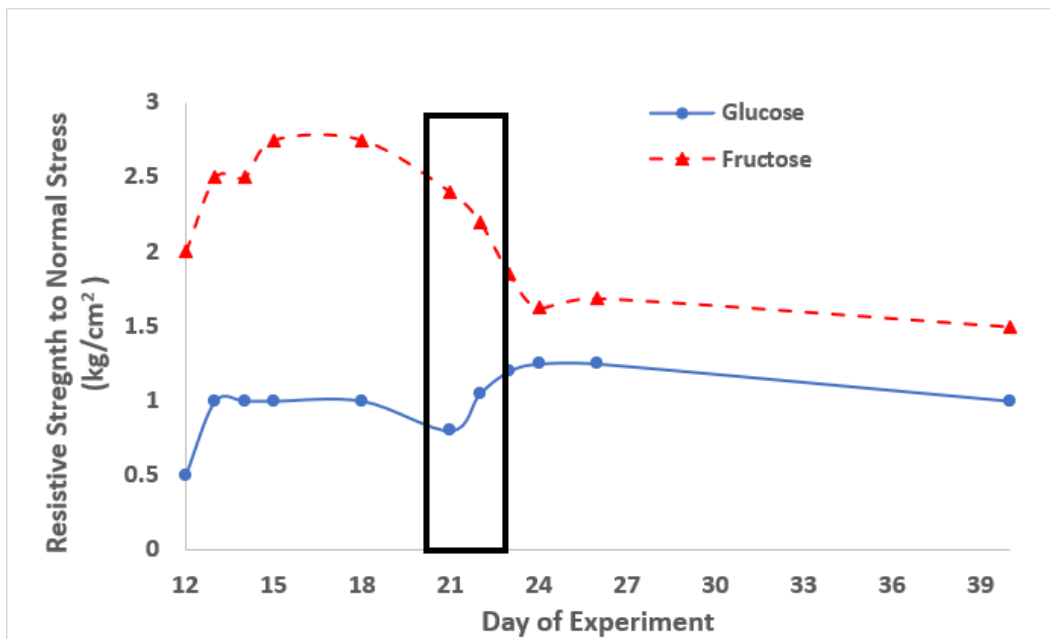


Figure 3-8: Comparison of resistive strength of the surface sediment to normal stress (penetrometer) for treatments including S2 with glucose (blue) and fructose (red), respectively, starting from Day 12 after commencement of MICP treatment. The black box is the section of the time during which the pods experienced heavy rainfall.

Dellanera Beach Tests

For the first series of beach tests, S1 and S2 were applied to the test plots at Dellanera Beach followed by a 14-day incubation period to allow the MICP reactions to occur. After this period, penetrometer measurements commenced. Penetrometer readings were taken every other day (6 sampling days) after the incubation period was completed. Readings were taken at three different points across each test plot as well as a control location outside the pods. The three readings from each point were averaged to give a representative value. The penetrometer results can be seen in Figure 3-9. The data indicate that the treated test plots did not show significant improvements in sediment resistive strength when compared to the natural sand on the beach. This was, in part, due to a massive rain event that occurred during the 14-day incubation period after the MICP solutions were applied during which the test plots were flooded, and any biological reactions were inhibited from occurring.

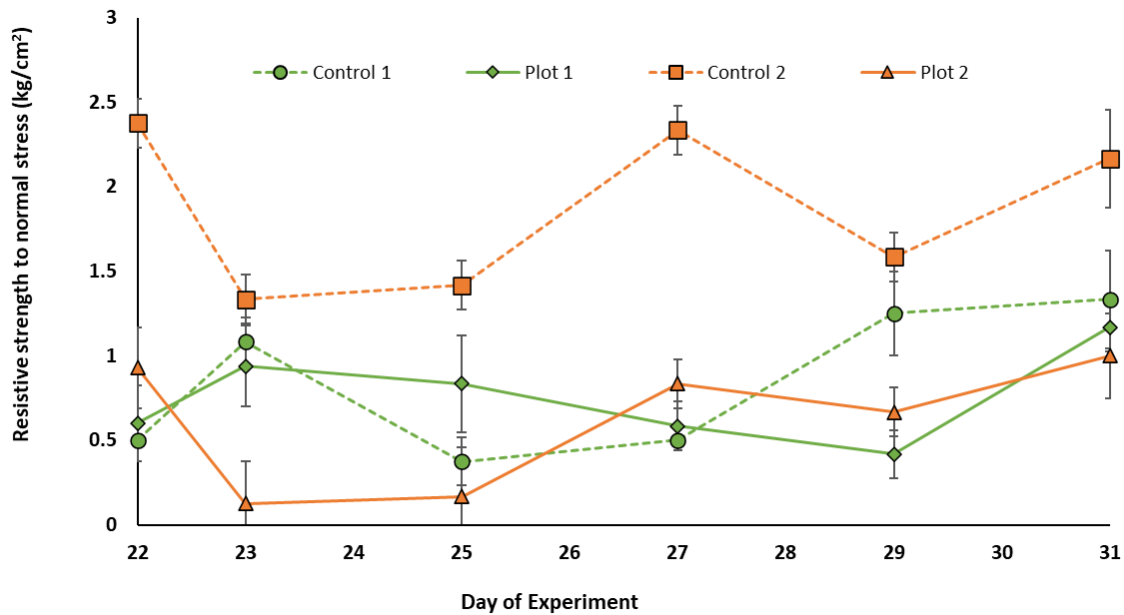


Figure 3-9: Measured resistive strength to normal stress (penetrometer) for MICP treated surface sediments during the first series of Dellanera Beach tests.

The second series of field tests featured the three different treatments (i) – (iii) applied to S2 as discussed in Section 3.2. The intent was to build on laboratory results further exploring the effect of:

- Use of yeast extract as growth medium for *S. pasteurii*
- Higher pH (~9) to aid the process of calcification
- Additional carbonate ions on the process of calcification.

The control treatment consisted of S2 with unaltered pH levels, however for both pH 9 (ii) and bicarbonate (iii) treatments, the pH of S2 was manually increased to ~9 using NaOH supplementation. In addition, 0.5 M of sodium bicarbonate was dissolved in S2 of the bicarbonate treatment. Weekly penetrometer measurements were taken to test the success and improvements in calcification for the different treatment options. Parallel penetrometer measurements were also performed on the beach outside the pods to obtain a baseline without any MICP solution applications. Figure 3-10 shows photos of the three test pods containing MICP treated sand at the three-week mark of data collection.



Figure 3-10: Photos of test pods at Dellanera Beach at week 3 of the experiment. From left to right: control plot, pH 9, bicarbonate.

Results indicate significantly higher ($p < 0.0283$, One-way ANOVA) resistance to normal stress in the sediment treated with the bicarbonate S2 compared to the control, the pH 9, and the “no treatment” options. The change in resistive strength to normal stress application over 5 weeks starting after completion of the MICP solution application is shown in Figure 3-11 for all four treatments. Penetrometer readings were taken over 5 weeks because resistive strength across the pods continued to change. It took 5 weeks to see a plateau in the strength values of the MICP treated sediment. Figure 3-11 shows that while the bicarbonate treatment showed higher strength values over the first two weeks, but it was not statistically significant. However, from Week 3 onward there was a significance in the higher penetrometer readings ($p < 0.0309$, One-way ANOVA). The bicarbonate treatment yielded about a 50% improved resistive strength during that time. No significant improvements in strength were measured in any of the other treatments.

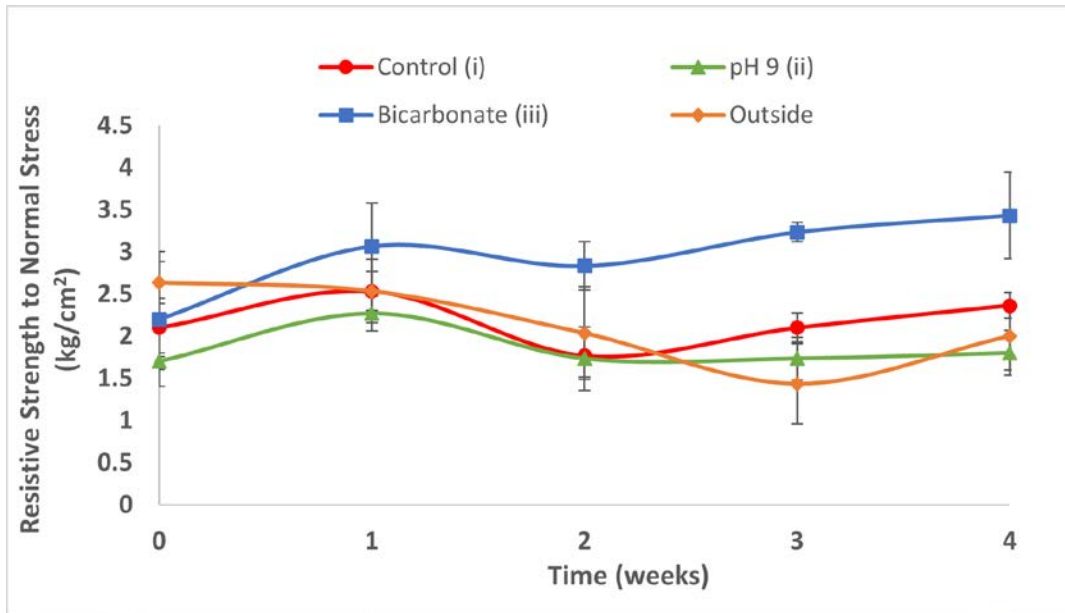


Figure 3-11: Measured resistive strength to normal stress (penetrometer) for MICP treated surface sediments (i)-(iii) and untreated sediment during the second series of Dellanera Beach tests.

3.4 Discussion

Several laboratory tests were conducted to determine the optimal parameters to induce MICP formation. Parameters tested include natural microbial community vs *S. pasteurii*, aerobic versus anaerobic conditions, presence and absence of organic carbon such as glucose or fructose, and sediment layering with different solutions during setup. Initial findings indicated that use of *S. pasteurii* under aerobic conditions with organic carbon and layering yielded better MICP formation. However, initial field tests highlighted the need for further optimization of the protocol to effectively apply and scale up the laboratory methodology to the field. Factors such as discrepancy in the proportional volume of MICP-inducing solutions required in contrast to laboratory protocols, humidity, groundwater levels and competition of the applied *S. pasteurii* with the indigenous bacteria in the sand may have influenced the fact that the initial field test did not produce calcification to the same extent as had been seen in the laboratory. In addition to refined field test strategies, it is also suggested to conduct larger scale laboratory experiments to isolate other factors resulting in the difference between lab and field application. This will help optimize the protocol for successful MICP formation in field applications and will inform future research.

The second series of field tests were performed to integrate the new findings from the laboratory, including the use of yeast extract as an optimal and cost-effective growth medium and the need to maintain a higher pH of ~ 9 to aid calcification. Moreover, the idea of an increased supply of carbonate ions supplied in the form of sodium bicarbonate to enhance calcification was successfully tested in the field. Simultaneously, this showed the potential of the MICP process to store inorganic carbon as calcium carbonate and hence aid in carbon sequestration. The pH 9 treatment showed no improvement in strength compared to the control or the outside suggesting that the pH levels may not be the only process impacting MICP, however, this might be primarily due to the impacts of heavy rain, which may have neutralized the pH in this treatment. The value of pH has been previously shown to play an important role in the success of MICP formation in field tests (Oualha et al., 2020). Significantly higher penetrometer readings in the bicarbonate treatment compared to all the treatments and the outside readings suggested that additional supply of carbonate ions improved the calcification enhancing the MICP process. This also implies that the additional inorganic carbon supplied in the form of sodium bicarbonate could have been stored as calcium carbonate underscoring the potential of the MICP process as a carbon-sequestering strategy. However, further experimentation is required to test and confirm this potential.

Interestingly, the pH of the solutions applied in the bicarbonate treatment was also adjusted to 9, but the discrepancy in relative strength between bicarbonate and pH-9 treatment raises questions about the influence of pH, underscoring the need for further laboratory experimentation to determine the underlying factors. Results showed that the MICP process was most effective when a 2-component approach was taken with a bacterial mixture (S1) and cementation mixture (S2). It was concluded that the most effective components of these mixtures are as follows: exponential phase culture of *S. pasteurii* in S1 and 1.5M CaCl₂ + 1M urea + 18 g/L fructose + 0.5M sodium bicarbonate in S2. Results also highlight that flooding of the MICP plots during the period of solution application and curation either caused by groundwater or rain can impact the success of the process. Shih et al. (2019) showed that increasing the relative density of soil by 60-80% might improve the solidification through MICP.

4 Coastal Engineering Applications of MICP

While MICP applications have mostly targeted soil liquefaction issues related to earthquake mitigation, there are many coastal engineering applications where MICP treatment of sediment may offer benefits via improved resistance to erosion. Applications can include beach and dune stabilization approaches where MICP treated sediment at the surface or underground strengthens the sediment matrix as mentioned in Chapter 1.2 and demonstrated in Chapter 3. The MICP process may also be used in conjunction with traditional coastal risk reduction systems to improve their performance. Geofabric bags filled with MICP-enhanced sand, for example, may reduce deformation of the bags as they are exposed under storm conditions and thus increase the level of protection. Rubble mounds and rock revetments could be enhanced in certain situations by partially or completely filling void spaces with MICP-enhanced sand to increase the level of resistance against rock slope or filter layer failure under hydrodynamic forcing (waves, currents, runoff, rain). The treated sediment could provide an alternative means to bind loose rock material together without the use of concrete. This may reduce the required design diameter or weight of the rock material or raise maximum slope limits.

One of the ultimate opportunities of locally sourced MICP-enhanced sediment for coastal engineering applications is the creation of submerged reefs, sills, and wave guiding structures to modify hydrodynamics and erosion trends at target locations. The benefit would be to eliminate the need to bring in expensive material from other places to construct the submerged feature. While this may require cofferdam structures built in the nearshore to allow for the aerobic MICP curing process to occur, once completed the hardened sediment structure can be flooded and function as intended.

Testing submerged MICP performance is beyond the scope of the current project. However, in addition to the laboratory and beach testing discussed in prior chapters, a limited number of preliminary experiments with geofabric bag samples and rock slopes was conducted to gain further insights into the use of MICP for coastal engineering applications.

4.1 Geofabric bags

Bags made of geofabric material are used for many coastal engineering applications including erosion protection and dewatering of dredged materials. As part of this project, geofabric bags are

tested as enclosures for MICP-treated material. The geofabric can provide stability and shape to the loose sediment while MICP is in process. Three different geotextile bag samples have been provided to the team for testing purposes. The bags measured approximately 0.9 x 0.9 x 0.9 m (3' x 3' x 3') and were tested outside next to the wooden field pods on both the TAMUG campus as well as the Dellanera beach, respectively. Each of the geofabric bags can hold sediment with a volume of approximately 0.73 m³ (26 ft³). Sediment is filled via a small opening through a fabric sleeve on the side of the bag.

The left panel of Figure 4-1 shows one of the tested geotextile bags made of a black felt type material (Mirafi S3200). It is a needle-punched non-woven geotextile composed of polypropylene fibers. The material thickness is 8.1 mm (320 mils) with a maximum opening size of 0.15 mm. The tensile strength of the Mirafi S3200 specified by the manufacturer is 3694 N (830 lbs). The second type is a geotextile bag made of green mesh material (GC1200MG). It is constructed of a high-strength woven geosynthetic base material and has a top layer of crimped fiber. The top layer allows for greater UV resistance and higher stability. The maximum opening size of the GC1200MG material is 0.30 mm. The manufacturer specifies its tensile strength in machine direction as 70 kN/m (100 lbs/in). The third type is a geotextile bag made of a black mesh material (GT500). It is composed of high-tenacity polypropylene yards woven into a stable network that prevents movement of the yards. The apparent opening size of the GT500 is 0.425 mm. This geotextile has a wide width tensile strength of 70 kN/m (400 lbs/in) in the machine direction.

The geotextile sample bags were filled with Galveston beach sand and treated using two different MICP solution application methods: (a) surficial spray treatment like the process used for the field plots and (b) application via button drippers where solutions are injected into the sand via openings in the fabric (see the right panel of Figure 4-1 for a photo). For each method both MICP-inducing solutions (S1 and S2) were applied three times a day over six days at the rate of 4 mL/s for 120 s. The geo-textile bags then underwent an incubation period of 14 days to allow bio-cementation to develop.



Figure 4-1: Photo of geo-synthetic bag made of Mirafi S3200 material. Left panel: empty bag prior to filling. Right panel: bag with evenly distributed button drippers inserted into the geofabric surface.

After the treatment cycle of 6 days and the 14-day curing period, the geofabric bags were visually inspected to see if any calcification had occurred. The sand inside them was still soft and did not appear to have any calcification. For further testing, the top layer of the bags was cut to expose a section of the treated sand. However, penetrometer readings did not indicate any increase in resistive strength for any of the sample bags or treatment options.

There were several factors that contributed to the poor performance of the MICP-treated geofabric bags. The most important factor is the difficulty in applying S1 and S2 to the sediment inside the bags. Surficial spraying proved difficult since microbes may not have been able to penetrate the fine fabric mesh in sufficient quantities. The button dripper application was intended to circumvent that issue but made even distribution of S1 and S2 throughout the bag problematic in addition to puncturing the bag surface which may compromise its integrity in an actual project application. Furthermore, severe weather including substantial rain events during the incubation period are thought to have contributed to the lack of observed calcification inside the geofabric bags much like for some of the open field test plots.

The conclusion of these preliminary tests with a very limited number of samples was that MICP enhancements do not seem feasible in conjunction with geofabric bags, but more experiments may be needed to provide further details on this topic.

4.2 Rock slope stability

Rock slopes are a common coastal protection measure. Multiple layers of rocks may be placed on top of a filter layer or the native soil to form a revetment. Rocks can also make up entire rubble mound structures. Options with or without concrete filler material exist. The objective is typically to dissipate wind wave or vessel wake energy and/or to reduce shoreline erosion. Design parameters for such systems include individual rock size and weight as well as the slope of the structure. MICP-enhanced sand may be used as cementing material partially filling the voids between rocks to improve rock slope performance without the need for concrete. This may increase the rock slope stability compared to loose rock placement and allow for larger slopes or smaller individual rocks to be utilized.

In a first attempt to test the feasibility of using MICP-enhanced sand as filler material to improve rock slope stability, a laboratory experiment investigating rock slope failure was performed. The basic idea was to record the movement of individual rocks on a slope consisting of three placed layers as the slope angle with the horizontal was increased all the way to complete failure. Three slope failure tests, each performed in duplicates, were conducted:

- (i) Rock slope without sand
- (ii) Rock slope with sand partially filling voids
- (iii) Rock slope with MICP-enhanced sand partially filling voids

A test consisted of increasing the rock slope in small increments and recording the number of individual rocks moving more than one nominal diameter as a function of slope. Results represent average values from the duplicate runs for each test, respectively.

To prepare the test setup, a base layer of about 90 granite rocks (94 and 91 for run 1 and 2, respectively) was glued to a horizontal 0.6 m x 0.6 m (2 ft x 2 ft) plywood sheet. The granite rocks used for the slope tests had a void ratio of 0.78 and the rocks were classified as angular in shape. The material density of granite is 2.7 g/cm^3 . Hinges on one end of the plywood sheet allowed it to be set at any angle between horizontal and vertical. Rocks were painted in different colors to simplify tracking of failure. For test (i), two additional rock layers were then individually placed on top of the first layer, minimizing void spaces (Figure 4-2). The number of rocks on the subsequent layer was 103 and 91 for each respective run. The third layer was comprised of 70 and

95 rocks for each run, respectively. The slope was increased until total failure occurred, i.e., when the top two layers of rocks had completely slid off the base layer. Two runs were done to account for variability in rock placement.



Figure 4-2: Slope Test Setup shown for the test involving rocks. The wire spool was used to increase the height (and therefore slope) of the rock matrix.

The same process was repeated with untreated sand partially filling the voids between the rock layers in test (ii). The plywood sheet and glued base layer of rocks were the same as for test (i). After the second layer of rocks had been placed by hand, sand was manually added into the void spaces by pouring it in from the top. This process was repeated after the third layer of rocks had been placed.

For test (iii) the same process as for test (ii) was used but this time MICP solutions (S1 and S2) were applied to the rock-sand matrix via surficial spraying. S1 was the same as used in the field experiments described in Chapter 3 and S2 consisted of 1M CaCl_2 + 1M urea + 18 g/L fructose + 0.5M sodium bicarbonate which was the most successful mix based on the Dellanera field experiments. The treatment cycle lasted for a period of six days with each matrix being treated

three times a day with 250 mL of each solution. Slope failure testing was conducted after an additional 2 weeks of curing to allow for the completion of the MICP process.

Results from test (i) indicated that the rocks experienced relatively sudden failure once a critical slope angle with the horizontal was reached. In run 1, about 20 rocks slid off the base layer at an angle of 38°. Total failure occurred at a slope angle of 45° where the top two layers of rocks all slid off the base layer. In run 2, about 40 rocks slid off the base layer and plywood sheet at an angle of 41°. Total failure for run 2 occurred at an angle of 49°. Between the initial movement and total failure angles, there were instances of only a few rocks failing until the final mass of rocks failed. The average total failure slope angle for the two runs was 47°.

For test (ii) the largest number of rock failures averaged over the two runs occurred around 42°. The angle of total failure occurred at an average angle of 51°. Run 1 experienced a single rock falling at an angle of 38°. This test also led to 55 rocks falling at an angle of 41° before total failure at 49°. In run 2, 2 rocks fell at an angle of 38° and about 60 rocks fell at an angle of 44° before total failure was experienced at a slope angle of 54°.

Test (iii) results showed significantly increased angles of total failure compared to the other tests. In run 1, the first 6 rocks slid off the base layer at a slope angle of 32°. Groups of about 5-10 rocks continued to slide off the base layer between slope angles of 36° and 51°. A group 60 rocks slid off the base layer at an angle of 56° and total failure occurred at a slope angle of 60°. In run 2, the first group of 7 rocks slid off the base layer at a slope angle of 34°. Groups or 2-3 rocks slid off the base layer consistently from slope angles of 36° to 61° except for 13 rocks sliding off at a slope angle of 38° and 15 rocks sliding off at an angle of 51°. Many the remaining rocks slid off the base layer at a slope angle of 66° however there were a few rocks from the additional layers remaining on top of the base layer at that angle. The slope continued to increase to allow for the last few remaining rocks to slide off leading to total failure occurring at a slope angle of 72°. On average, total failure occurred at an angle of 66° (average of 60° and 72° from the two individual runs).

After test (iii) had been completed, the bottom layer of rocks and remaining MICP-enhanced sand showed visual evidence of calcification, providing further proof that the MICP process had worked. Figure 4-3 shows an image of the observed calcification after test (iii) where a few pockets of visible sodium bicarbonate deposits can also be seen indicating that further optimization of the S2 mixture is possible.



Figure 4-3: Visual evidence of calcification in MICP-treated rock-sand matrix after complete slope failure of test (iii). Calcification is visible as an off-white color while remaining pockets of sodium bicarbonate deposits are bright white.

A graphical representation of all data collected as part of the rock slope failure experiment is given in Figure 4-4 where slope angle is shown as a function of the number of failed rocks. This experiment proved to be very valuable in quantifying the potential benefit of MICP in improving rock slope stability. While initiation of individual rock failures in the top layer happened at similar slope angles across all tests, the angle at which total slope failure occurred was significantly increased for the MICP-enhanced setup. The angle of total failure for test (iii) with MICP treatment indicated an increase in average total failure angle of 40% and 29% compared to the plain rock slope (i) and rock and untreated sand slope (ii), respectively. These tests show that further improvements to the MICP application process to mixed rock-sand slopes can lead to significant stability improvements if the observed calcification process is achieved throughout all rock-sand layers. Further rock-sand slope tests are planned in the future to solidify these findings.

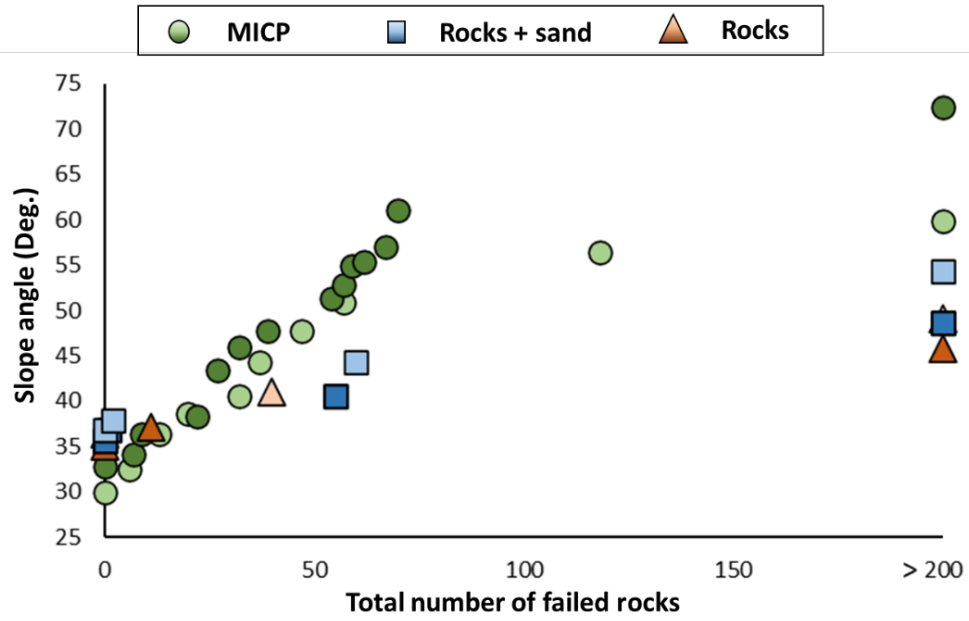


Figure 4-4: Measured slope angle versus total number of failed rocks for all runs of tests (i), (ii), and (iii). Values for duplicates in each test are indicated by respective lighter and darker shade symbols.

5 Hydrodynamics and Sediment Analysis

Hydrodynamic data near the proposed project field site was collected during Hurricane Laura to provide some in situ information that may be helpful for design and modeling purposes. These data had already been shared in the midterm progress report for this project but are presented here again for completeness. Laura made landfall near Cameron on the Louisiana Coast on August 27, 2020 as a high-end category 4 hurricane (150 mph, 937 mBar). Data collection at the project site happened over the 7-day period between August 25, 2020 and September 1, 2020. Data was collected by a Nortek Vector acoustic Doppler velocimeter (ADV) and an RBR SoloD|Wave pressure transducer and consisted of 3-D velocity and pressure at a fixed point in the water column. The instruments were mounted on a goal post frame on the seaward side of the second sand bar in the surf zone just offshore of the Dellanera RV park on Galveston Island (approximately 1.5 m water depth during installation under normal conditions). In the following, data collected by the ADV including an internal pressure sensor are presented. The sampling rate was set at 8 Hz for continuous sampling throughout the deployment.

Figure 5-1 shows the recorded raw pressure (top panel) and the two horizontal velocity components (bottom panel) for the entire time series (over 3.5 million samples). The pressure is given in dbar and ranges from approximately 0.4 to 3.5 dbar. Changes in pressure given in dbar are roughly equivalent to changes in water level given in m. The raw pressure signal clearly shows increases in water level due to the hurricane as well as water level fluctuations due to tides. A ten-minute running average time series is indicated by the blue line and is used to show the underlying water level variations due to storm surge and tides. For wave analysis, these low-frequency water level fluctuations are subtracted from the total pressure time series. It can also be seen from the top panel of Figure 5-1 that wave heights (the fluctuations around the local mean) increase during hurricane impact as well as during high tide. During low tide, wave heights are smaller. This is typical of surf zone locations where higher water levels tend to shift wave breaking further landward.

The bottom panel of Figure 5-1 shows the cross-shore and alongshore velocity components, respectively. Maximum cross-shore velocity fluctuations were measured during storm impact with changes between -1.8 m/s and 2.0 m/s within several orbital wave cycles possible. During storm impact the predominant alongshore current was toward the west (positive). With passage of the

storm the average alongshore current direction reversed toward the east (negative) as indicated by the clear shift seen in the alongshore velocity component (red line) in the bottom panel of Figure 5-1 past the peak of the storm.

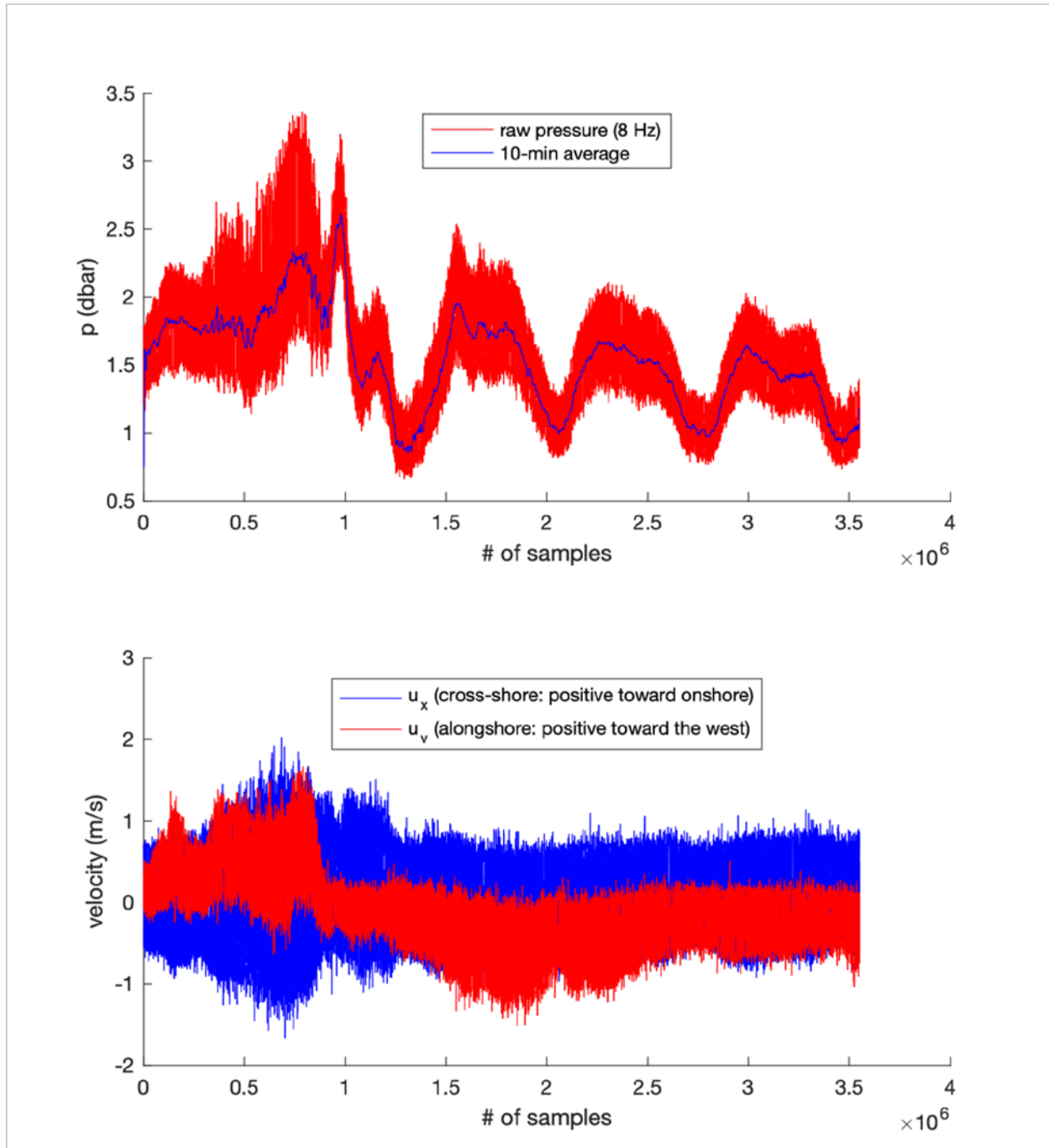


Figure 5-1: Top panel: Measured pressure (raw and 10-min average) in the surf zone near Dellanera RV park on Galveston Island. Bottom panel: Cross-shore (blue) and alongshore (red) velocity components measured at the same location. The total duration was about 7 days including landfall of Hurricane Laura.

Figure 5-2 shows two zoomed in 100-second sections of Figure 5-1. The left panels show 100 seconds of measured data around the peak of the storm. The right panels show 100 seconds of measured data during low tide conditions after the storm. Note that the y-axis scales have been kept the same to simplify visual comparison between the two time periods. The nonlinear breaking wave signature with accentuated peaks and flattened troughs is apparent in the top left panel. The bottom left panel clearly shows the rapid swings between large negative (offshore) and large positive (onshore) velocity during wave passage. Water level fluctuations and velocities are much reduced during calm conditions (right panels).

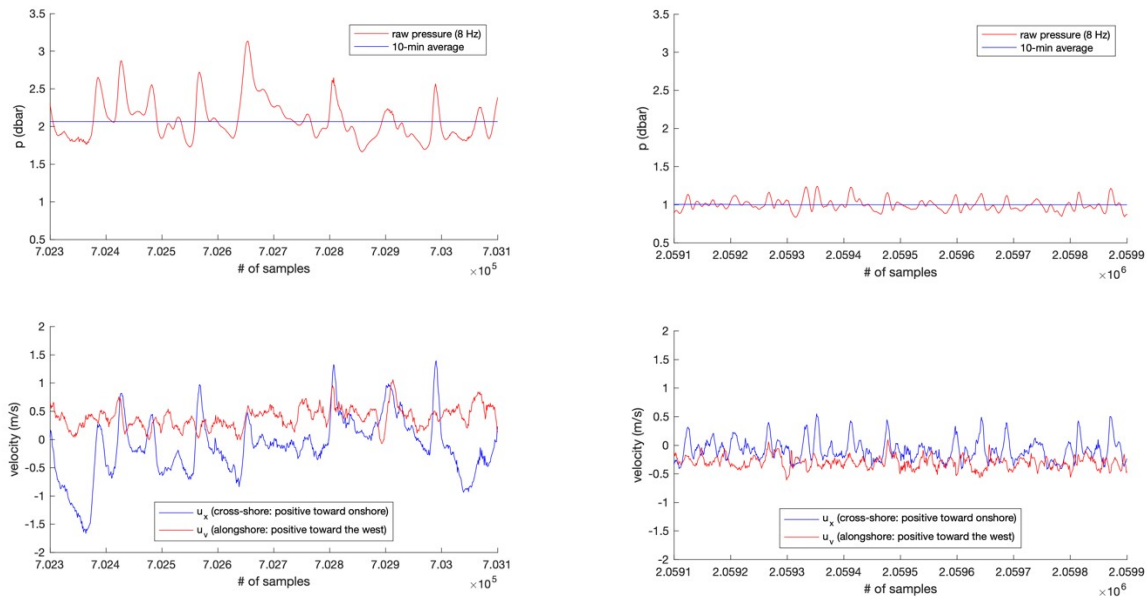


Figure 5-2: Left panels: 100-second excerpt of pressure and velocity time series during storm impact. Right panels: 100-second excerpt of pressure and velocity time series during low tide calm conditions.

The raw pressure data was further processed to yield hourly wave statistics. For each hour segment of data, the first 10 minutes were used to calculate wave statistics after removing the mean from the raw pressure data. An up-crossing method was employed to isolate individual waves in the time series. Significant wave height was then calculated by sorting these waves from highest to lowest and taking the average of the highest 1/3 of these waves. Figure 5-3 shows time series of hourly significant wave height, H_s , maximum wave height, H_{max} , significant wave period, T_s , and peak period, T_p , respectively. Maximum wave height during the peak of the storm reached up to

1.4 m at this surf zone location, keeping in mind that these are waves that have already broken, are reforming, or are in the process of breaking. The largest significant wave height during the storm was just below 1 m. Wave heights in the surf zone tend to reduce during lower water levels since breaking is enhanced. This can be seen in the top panel of Figure 5-3 where both H_s and H_{max} drop as tide levels go down and increase as tide levels go up again. The significant wave period, T_s , ranges from 4 s during normal conditions to 12 s during storm conditions with peak period, T_p , during the storm even higher (16 s and above). Due to the difficult measuring conditions in the surf zone, some unrealistic peak periods during rough conditions were eliminated from the data set.

Results from two surface sediment sampling campaigns carried out near the project site at Dellanera RV Park on Galveston Island are presented. Six Samples were collected on 7/15/2020 (Campaign C1) and eight samples were collected on 9/1/2020 (Campaign C2), five days after Hurricane Laura had made landfall along the Louisiana coast. Figure 5-4 shows location details of all samples collected during the two campaigns. The yellow pins mark the base locations for C1 and C2 with coordinates of Lat./Long. $29^{\circ}14'20.99''$ N/ $94^{\circ}52'29.73''$ W and $29^{\circ}14'22.93''$ N/ $94^{\circ}52'26.26''$ W, respectively.

Individual samples were collected from the first two surf zone troughs (S1-S2), on the first two surf zone crests (S3-S4), and on the dry beach (S5-S6) for each campaign with an extra two samples collected near the hydrodynamic instrument locations for C2 (S7-S8; red pins in Figure 5-4).

Grain size analysis was carried out at the TAMUG geotechnical engineering laboratory using a drying oven and sieve shaker towers (sieve sizes: #35, #70, #120, #140, #170, #200, #230). Average grain size distribution plots for Campaign 1 and 2 are given in Figure 5-5 and Figure 5-6, respectively. The results for both campaigns indicate mostly poorly graded, fine sand with a median diameter of approximately $D_{50} = 0.16$ mm on average. Some samples included a shell or shell fragments larger than the #35 sieve opening accounting for the percent finer value at the #35 sieve to be below 100%. Specific shell fragment sizes were not determined but their respective weights are included in the analysis and are reflected in the percentages of sediment fractions reported.

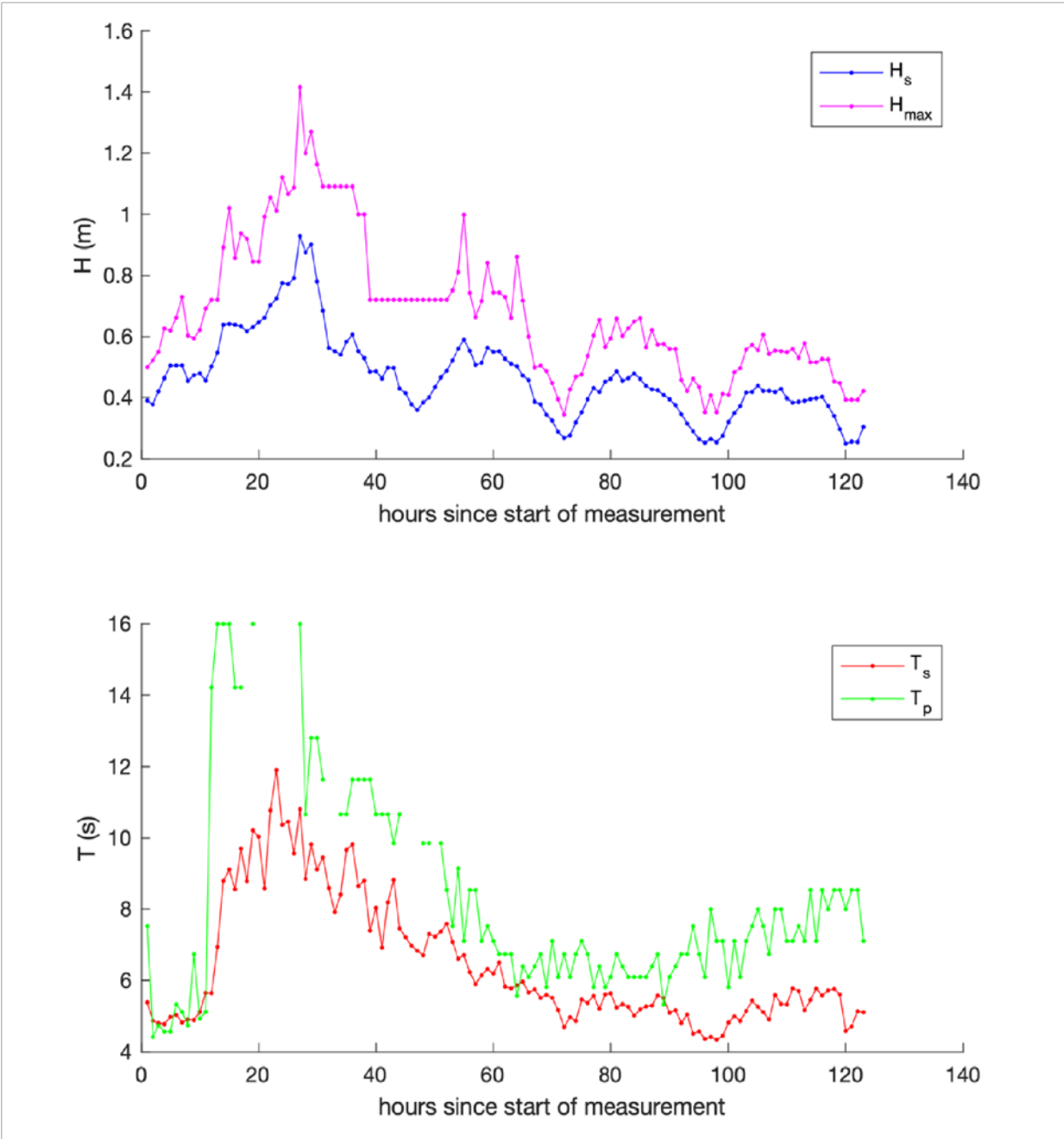


Figure 5-3: Top panel: Hourly wave height (significant and maximum) during the 7-day deployment. Bottom panel: Hourly wave period (significant and maximum) during the same time.

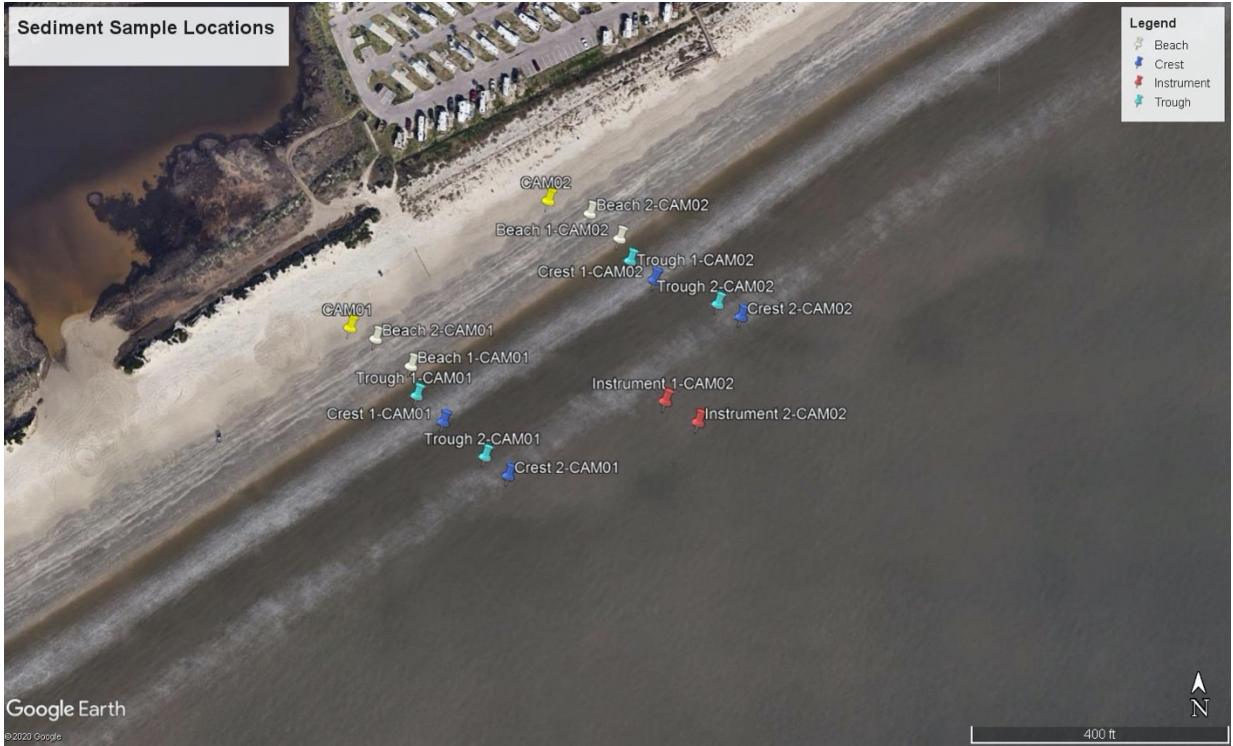


Figure 5-4: Google Earth image of the beach near Dellanera RV Park including place marks of individual sampling locations for two sediment sampling campaigns.

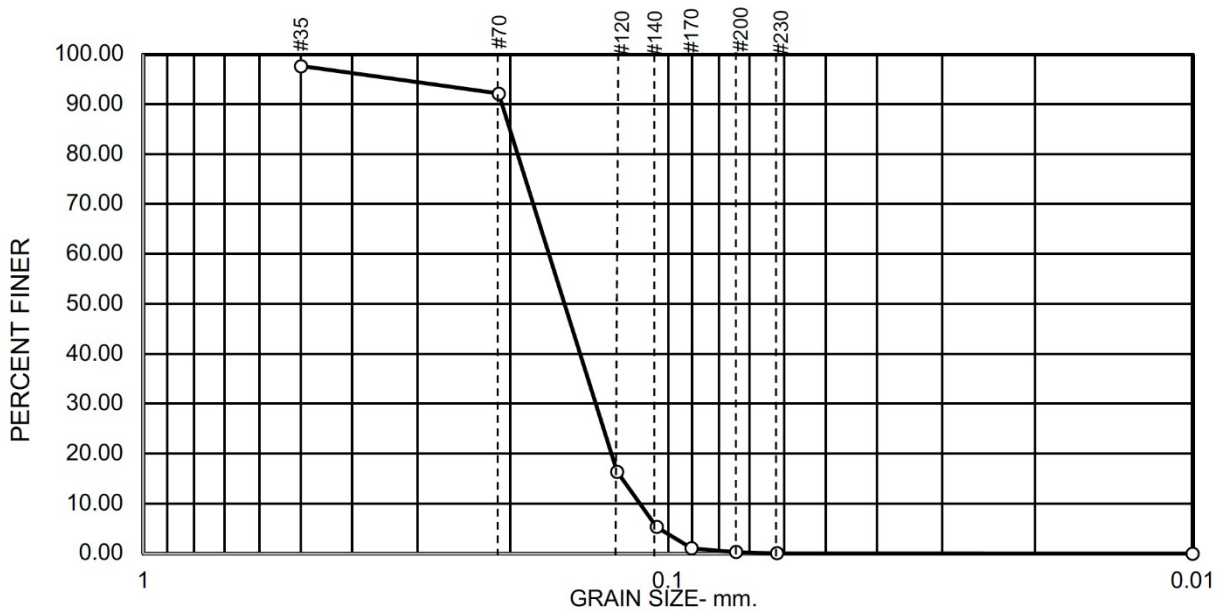


Figure 5-5: Average grain size distribution for Campaign 1.

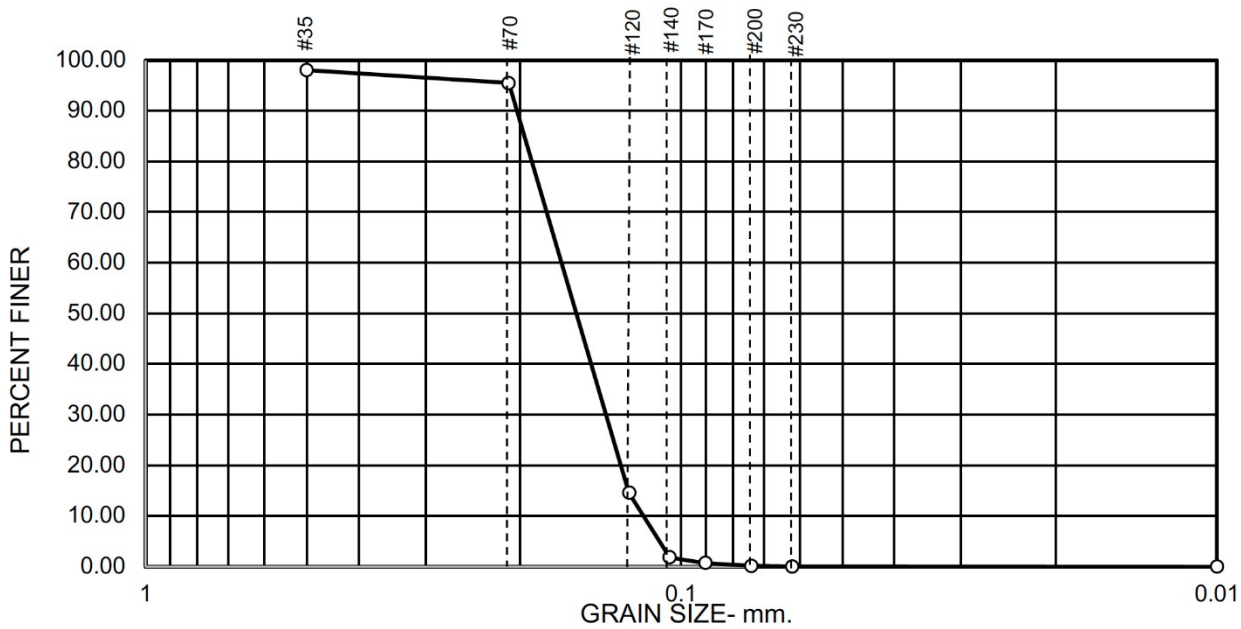


Figure 5-6: Average grain size distribution for Campaign 2.

6 Conclusions and Recommendations

Microbially-induced calcium carbonate precipitation (MICP) is an integral part of a process that allows naturally occurring microbes to bind sediment grains together. The increase of cemented bonds between individual grains leads to a more stable sediment matrix. Depending on the level of cementation, MICP treated sediment displays increased resistance to erosion. This report details findings from a TAMU/TEES study on the controlled use of the MICP process to enhance coastal flood risk reduction and erosion mitigation systems. Through laboratory and field testing, the study determined the optimal setup and composition of MICP inducing solutions for application in Galveston Island coastal settings. Additional experiments on MICP use in conjunction with geofabric bags (or “geotubes”) and rock revetment slopes were conducted. The feasibility of using MICP treated sediment for beach, dune, or submerged sill/reef stabilization were discussed based on experiment outcomes.

The MICP process is induced by subjecting sediment to two different solutions. Solution S1 (bacterial mixture) introduces the microbes while solution S2 (cementation mixture) introduces the components needed for the microbe population to perform biochemical reactions required for cementation. In the laboratory, the strongest calcification was observed in autoclaved sediment samples treated with S1 containing *S. pasteurii* and S2 containing calcium chloride (CaCl₂), urea, and glucose under aerobic conditions. It was difficult to reproduce similar calcification results in the field due to added uncertainty in environmental conditions (e.g., rain events, competing microbes, application method, etc.). Nonetheless, resistance to applied normal stress approximately doubled in field plots treated with bicarbonate, fructose as substitute for glucose, and yeast extract as a cheaper substitute for marine broth compared to untreated plots of sand.

A summary of the main findings is given here:

- Aerobic conditions are preferred for MICP to form.
- The addition of glucose improved MICP formation, but fructose was found to be a viable, more cost-efficient substitute.
- A layering approach to MICP treatment of a sand column has been found beneficial to the formation of calcification. Here layers of treated and untreated sand are alternated prior to continued supply of MICP solutions from the surface.

- Yeast extract proved to be the optimal choice of growth medium both in terms of biomass productivity and cost-efficiency compared to the traditionally used marine broth since it led to 2.5-times higher growth of *S. pasteurii* (at 20 g/L).
- Increased bacterial growth was observed in the absence of urea in a modified S2 combined with a neutral pH level suggesting that the urease activity is causing the pH of the medium to turn acidic which may negatively impact calcification. Further testing on the impact of pH level on the MICP process is suggested to determine optimal values.
- Results from the field tests showed that the MICP process was most effective when a 2-component approach was taken with a bacterial mixture (S1) and cementation mixture (S2). It was concluded that the most effective components of these mixtures are as follows: exponential phase culture of *S. pasteurii* in S1 and 1.5M CaCl₂ + 1M urea + 18 g/L fructose + 0.5M sodium bicarbonate in S2. This treatment led to significantly increased penetrometer readings. Apart from the enhanced calcification and improved resistance to normal stress of the treated sediment, the additional inorganic carbon supplied in the form of sodium bicarbonate indicates that there may be a pathway to use the MICP process as a carbon-sequestering strategy.
- The combination of geofabric bags and MICP treated sand did not produce any improved sediment characteristics, in part due to the limited number of trials available, but also due to the adverse weather conditions during field testing, and permeability issues of the geofabric for the microbes.
- Total failure slope angles were increased for slopes made up of a matrix of rocks and MICP enhanced sand versus plain rock slopes (by up to 40%) when the most optimal MICP solutions found from other tests were used for treatment. This aspect of MICP use in coastal risk reduction systems has the potential to increase cost-efficiency for such systems (reduced space requirements, reduced rock sizes, etc.) and should be investigated further.

This one-year study on MICP applicability to coastal flood-risk mitigation measures has produced some promising results but has also highlighted the fact that more time and research is needed to upscale the findings and make them applicable for project design. Based on the findings to date it is recommended to continue laboratory and field testing and optimization of the MICP process to

build on the progress made so far. While application of MICP enhancements to subaerial sediment in a beach-dune system seems promising, the subaqueous application for submerged sill and reef creation will be more challenging due to the need for aerobic conditions during MICP formation which may require substantial coffer dam structures and dewatering systems to be in place in the nearshore for several weeks until the cementation process has been completed.

Field measurements of hydrodynamics (waves, current velocities) during calm and energetic conditions in the surf zone near the proposed field site have been collected and analyzed along with surface sediment grab samples on the beach and in the surf zone. Results from the analysis of these data are presented in this report and can be used to aid in the submerged reef design process.

7 References

- Badiee, H., Sabermahani, M., Tabandeh, F., and Javadi, A. S. (2019). Application of an indigenous bacterium in comparison with *Sporosarcina pasteurii* for improvement of fine granular soil. *International Journal of Environmental Science and Technology*, 16(12), 83898400.
- Bonato J., Heineck K., Thomé A., DallAgnol B., and Garbin G.R. (2016). Bio-nanocementation to evaluate soil mechanical resistance. *Geo-Chicago 2016*, 430–440. <https://doi.org/10.1061/9780784480120.044>
- Chiew, Y. M. (1992). Scour protection at bridge piers. *Journal of Hydraulic Engineering*, 118(9), 1260-1269.
- Chu, J., Stabnikov, V., and Ivanov, V. (2012). Microbially induced calcium carbonate precipitation on surface or in the bulk of soil. *Geomicrobiology Journal*, 29(6), 544–549. <https://doi.org/10.1080/01490451.2011.592929>
- Cuthbert, M.O., McMillan, L.A., Handley-Sidhu, S., Riley, M.S., Tobler, D.J., and Phoenix, V.R. (2013). A field and modeling study of fractured rock permeability reduction using microbially induced calcite precipitation. *Environmental Science & Technology*, 47(23), 13637-13643.
- Do J., Montoya B.M., and Gabr M.A. (2020). Microbially induced carbonate precipitation process for soil improvement adjacent to model pile by innovative delivery system. *GeoCongress 2020*, 188–195. <https://doi.org/10.1061/9780784482834.021>
- Do, J., Montoya, B.M., and Gabr, M.A. (2019). Debonding of microbially induced carbonate precipitation-stabilized sand by shearing and erosion. *Geomechanics and Engineering*, 17(5), 429–438. <https://doi.org/10.12989/GAE.2019.17.5.429>
- Eiteman, M.A. and Ramalingam, S. (2015). Microbial production of lactic acid. *Biotechnology Letters*, 37(5), 955–972. <https://doi.org/10.1007/s10529-015-1769-5>
- Feng K. and Montoya B.M. (2017). Quantifying level of microbial-induced cementation for cyclically loaded sand. *Journal of Geotechnical and Geoenvironmental Engineering*, 143(6), 06017005. [https://doi.org/10.1061/\(ASCE\)GT.1943-5606.0001682](https://doi.org/10.1061/(ASCE)GT.1943-5606.0001682)
- Ferris, F.G., Phoenix, V., Fujita, Y., and Smith, R.W. (2004). Kinetics of calcite precipitation induced by ureolytic bacteria at 10 to 20°C in artificial groundwater. *Geochimica et Cosmochimica Acta*, 68(8), 1701–1710. [https://doi.org/10.1016/S0016-7037\(03\)00503-9](https://doi.org/10.1016/S0016-7037(03)00503-9)
- Fujita, Y., Ferris, F.G., Lawson, R.D., Colwell, F.S., and Smith, R.W. (2000). Subscribed content calcium carbonate precipitation by ureolytic subsurface bacteria. *Geomicrobiology Journal*, 17(4), 305–318. <https://doi.org/10.1080/782198884>
- Fujita, Y., Taylor, J.L., Gresham, T.L., Delwiche, M.E., Colwell, F.S., McIning, T.L., Petzke, L.M. and Smith, R.W. (2008). Stimulation of microbial urea hydrolysis in groundwater to enhance calcite precipitation. *Environmental Science and Technology*, 42, 3025-3032.

- Gebru, K. A., Kidanemariam, T. G., & Gebretinsae, H. K. (2021). Bio-cement production using microbially induced calcite precipitation (MICP) method: A review. *Chemical Engineering Science*, 238, 116610.
- Ghasemi P. and Montoya B.M. (2020). Field application of the microbially induced calcium carbonate precipitation on a coastal sandy slope. *Geo-Congress 2020*, 141–149. <https://doi.org/10.1061/9780784482834.016>
- Ghasemi P., Zamani A., and Montoya B.M. (2019). The effect of chemical concentration on the strength and erodibility of MICP treated sands. *Geo-Congress 2019*, 241–249. <https://doi.org/10.1061/9780784482117.024>
- Gomez, M.G., Martinez, B.C., De Jong, J.T., Hunt, C.E., deVlaming, L.A., Major, D.W., and Dworatzek, S.M. (2015). Field-scale bio-cementation tests to improve sands. *Proceedings of the Institution of Civil Engineers - Ground Improvement*, 168(3), 206–216. <https://doi.org/10.1680/grim.13.00052>
- Gomez, M.G. (2017). Up-scaling of bio-cementation soil improvement using native soil microorganisms [Ph.D., University of California, Davis]. <https://search.proquest.com/docview/1906984165/abstract/DB602C6E798B4808PQ/1>
- Jain, S. and Arnepalli, D.N. (2019). Biochemically induced carbonate precipitation in aerobic and anaerobic environments by *Sporosarcina pasteurii*. *Geomicrobiology Journal*, 36(5), 443–451.
- Kortbawi M.E., Ziotopoulou K., Gomez M.G., and Lee M. (2019). Validation of a bounding surface plasticity model against the experimental response of (bio-) cemented sands. *GeoCongress 2019*, 197–207. <https://doi.org/10.1061/9780784482100.021>
- Landa-Marbán, D., Tveit, S., Kumar, K., & Gasda, S. E. (2021). Practical approaches to study microbially induced calcite precipitation at the field scale. *International Journal of Greenhouse Gas Control*, 106, 103256.
- Lesley A., Warren, F.G.F., Patricia A.M., and Nagina P. (2001). Microbially mediated calcium carbonate precipitation: Implications for interpreting calcite precipitation and for solid-phase capture of inorganic contaminants. *Geomicrobiology Journal*, 18(1), 93–115. <https://doi.org/10.1080/01490450151079833>
- Li, M., Wen, K., Li, Y., & Zhu, L. (2018). Impact of oxygen availability on microbially induced calcite precipitation (MICP) treatment. *Geomicrobiology Journal*, 35(1), 15–22.
- Marín, S., Cabestrero, O., Demergasso, C., Olivares, S., Zetola, V., & Vera, M. (2021). An indigenous bacterium with enhanced performance of microbially-induced Ca-carbonate biomineralization under extreme alkaline conditions for concrete and soil-improvement industries. *Acta Biomaterialia*, 120, 304–317.
- Mondal, S. and Ghosh, A.D. (2019). Review on microbial induced calcite precipitation mechanisms leading to bacterial selection for microbial concrete. *Construction and Building Materials*, 225, 67–75.

- Montoya, B.M., Do J., and Gabr M.A. (2018). Erodibility of microbial induced carbonate precipitation-stabilized sand under submerged impinging jet. *IFCEE 2018*, 19–28. <https://doi.org/10.1061/9780784481592.003>
- Montoya, B.M., De Jong, J.T., and Boulanger, R.W. (2014). Dynamic response of liquefiable sand improved by microbial-induced calcite precipitation. In *Bio- and Chemo-Mechanical Processes in Geotechnical Engineering* (Vol. 1–0, pp. 125–135). ICE Publishing. <https://doi.org/10.1680/bcmpge.60531.012>
- Montoya, B.M. (2012). Bio-mediated soil improvement and the effect of cementation on the behavior, improvement, and performance of sand [Ph.D., University of California, Davis]. <https://search.proquest.com/docview/1023379941?pq-origsite=gscholar>
- Mori, D., & Uday, K. V. (2021). A review on qualitative interaction among the parameters affecting ureolytic microbial-induced calcite precipitation. *Environmental Earth Sciences*, 80(8), 1-20.
- Mortensen, B.M., Haber, M.J., DeJong, J.T., Caslake, L.F., and Nelson, D.C. (2011). Effects of environmental factors on microbial induced calcium carbonate precipitation. *Journal of Applied Microbiology*, 111(2), 338–349. <https://doi.org/10.1111/j.1365-2672.2011.05065.x>
- Nafisi A. and Montoya B.M. (2018). A new framework for identifying cementation level of MICP-treated sands. *IFCEE 2018*, 37–47. <https://doi.org/10.1061/9780784481592.005>
- Nafisi A., Montoya B.M., and Evans T.M. (2020). Shear strength envelopes of biocemented sands with varying particle size and cementation level. *Journal of Geotechnical and Geoenvironmental Engineering*, 146(3), 04020002. [https://doi.org/10.1061/\(ASCE\)GT.19435606.0002201](https://doi.org/10.1061/(ASCE)GT.19435606.0002201)
- Nafisi A., Safavizadeh S., and Montoya B.M. (2019). Influence of microbe and enzyme-induced treatments on cemented sand shear response. *Journal of Geotechnical and Geoenvironmental Engineering*, 145(9), 06019008. [https://doi.org/10.1061/\(ASCE\)GT.1943-5606.0002111](https://doi.org/10.1061/(ASCE)GT.1943-5606.0002111)
- Nafisi, A., Khoubani, A., Montoya, B.M., and Evans, T.M. (2018). The effect of grain size and shape on mechanical behavior of MICP sand I: experimental study. *Proceedings of the 11th National Conference in Earthquake Engineering*, 9.
- Omoregie, A.I., Khoshdelnezamiha, G., Senian, N., Ong, D.E.L., and Nissom, P.M. (2017). Experimental optimisation of various cultural conditions on urease activity for isolated *Sporosarcina pasteurii* strains and evaluation of their biocement potentials. *Ecological Engineering*, 109, 65-75.
- Oualha, M., Bibi, S., Sulaiman, M., & Zouari, N. (2020). Microbially induced calcite precipitation in calcareous soils by endogenous *Bacillus cereus*, at high pH and harsh weather. *Journal of environmental management*, 257, 109965.
- Phillips, A.J., Cunningham, A.B., Gerlach, R., Hiebert, R., Hwang, C., Lomans, B.P., ... and Spangler, L. (2016). Fracture sealing with microbially-induced calcium carbonate precipitation: A field study. *Environmental Science & Technology*, 50(7), 4111-4117.

- Phillips, A.J., Troyer, E., Hiebert, R., Kirkland, C., Gerlach, R., Cunningham, A.B., ... & Esposito, R. (2018). Enhancing wellbore cement integrity with microbially induced calcite precipitation (MICP): a field scale demonstration. *Journal of Petroleum Science and Engineering*, 171, 1141-1148.
- Rajasekar, A., Moy, C. K., Wilkinson, S., & Sekar, R. (2021). Microbially induced calcite precipitation performance of multiple landfill indigenous bacteria compared to a commercially available bacteria in porous media. *Plos one*, 16(7), e0254676.
- Safavizadeh S., Montoya B.M., Gabr M.A., & Knappe D.R.U. (2019). Factors affecting the kinetics of urea hydrolysis via *Sporosarcina pasteurii*. *Geo-Congress 2019*, 105–114. <https://doi.org/10.1061/9780784482148.011>
- Seifan, M. and Berenjian, A. (2019). Microbially induced calcium carbonate precipitation: A widespread phenomenon in the biological world. *Applied Microbiology and Biotechnology*, 103(12), 4693–4708. <https://doi.org/10.1007/s00253-019-09861-5>
- Shanahan C. and Montoya B.M. (2016). Erosion reduction of coastal sands using microbial induced calcite precipitation. *Geo-Chicago 2016*, 42–51. <https://doi.org/10.1061/9780784480120.006>
- Shih, D. S., Lai, T. Y., & Hsu, Z. M. (2019). Applying biomineralization technology to study the effects of rainfall induced soil erosion. *Water*, 11(12), 2555.
- Sun, X., Miao, L., and Wang, C. (2019). Glucose addition improves the bio-remediation efficiency for crack repair. *Materials and Structures*, 52(6), 1-18.
- Terzis, D., Bernier-Latmani, R., and Laloui, L. (2016). Fabric characteristics and mechanical response of bio-improved sand to various treatment conditions. *Géotechnique Letters*, 6(1), 50–57. <https://doi.org/10.1680/jgele.15.00134>
- Van Paassen, L.A. (2009). Biogrout, ground improvement by microbial induced carbonate precipitation [Ph.D., TU Delft]. <http://resolver.tudelft.nl/uuid:5f3384c4-33bd-4f2a-86417c665433b57b>
- Verduyn, C., Postma, E., Scheffers, W.A., and van Dijken, J. P. (1990). Physiology of *Saccharomyces cerevisiae* in anaerobic glucose-limited chemostat cultures. *Microbiology*, 136(3), 395–403. <https://doi.org/10.1099/00221287-136-3-395>
- Zamani A., and Montoya B.M. (2016). Permeability reduction due to microbial induced calcite precipitation in sand. *Geo-Chicago 2016*, 94–103. <https://doi.org/10.1061/9780784480120.011>
- Zamani A., and Montoya B.M. (2017). Shearing and hydraulic behavior of MICP treated silty sand. *Geotechnical Frontiers 2017*, 290–299. <https://doi.org/10.1061/9780784480489.029>
- Zamani, A., and Montoya, B.M. (2019). Undrained cyclic response of silty sands improved by microbial induced calcium carbonate precipitation. *Soil Dynamics and Earthquake Engineering*, 120, 436–448. <https://doi.org/10.1016/j.soildyn.2019.01.010>

Zamani, A., Montoya, B.M., and Gabr, M.A. (2019). Investigating challenges of in situ delivery of microbial-induced calcium carbonate precipitation (MICP) in fine-grain sands and silty sand. *Canadian Geotechnical Journal*, 56(12), 1889–1900. <https://doi.org/10.1139/cgj-20180551>